Analysis and Experimentation of a Single Stage Travelling-wave Thermoacoustic Engine

Morathanne Dewayalage Anuradha Wickramasinghe

218060H

Master of Science (Major Component Research)

Department of Mechanical Engineering

Faculty of Engineering

University of Moratuwa

Sri Lanka

March 2025

Analysis and Experimentation of a Single Stage Travelling-wave Thermoacoustic Engine

Morathanne Dewayalage Anuradha Wickramasinghe

218060H

Thesis/Dissertation submitted in partial fulfillment of the requirements for the degree
Master of Science (Major Component Research)

Department of Mechanical Engineering
Faculty of Engineering

University of Moratuwa
Sri Lanka

March 2025

DECLARATION

I declare that this is my own work, and this thesis/dissertation does not incorporate without acknowledgement any material previously submitted for a degree or diploma in any other University or Institute of higher learning and to the best of my knowledge and belief it does not contain any material previously published or written by another person except where the acknowledgement is made in the text. I retain the right to use this content in whole or part in future works (such as articles or books).

Signature: Date: 06/03/2025

The above candidate has carried out research for the PhD/MPhil/Masters thesis/dissertation under my supervision. I confirm that the declaration made above by the student is true and correct.

Name of Supervisor	Signature of the Supervisor	Date
Dr. MMID Manthilake		07/03/2025
Dr. MA Wijewardane		07/03/2025
Dr. RACP Ranasinghe		08/03/2025

DEDICATION

This thesis is humbly dedicated to the most important people in my life, my cherished parents who have guided me throughout this journey. Your guidance and unwavering support have been my motivation.

ACKNOWLEDGEMENT

I deeply thank my beloved parents for their unwavering support, encouragement, and sacrifices throughout this journey. Your belief in my abilities and constant motivation has been my guiding light, inspiring me to strive for excellence in every endeavor.

To my dear wife, your patience, understanding, and unwavering belief in me have been the pillars of strength during the challenging times of this study. I am forever grateful for your love and companionship.

I am immensely thankful to my steam supervisors for their invaluable guidance, expert advice, and continuous encouragement throughout this research. Your mentorship, wisdom, and constructive feedback have been instrumental in shaping my ideas and refining my work, enabling me to reach new heights of academic excellence.

A heartfelt appreciation goes to the dedicated staff of the workshop, die and mold center, production laboratory, and refrigeration and air conditioning laboratory in the Department of Mechanical Engineering for their invaluable assistance, technical expertise, necessary resources, facilities, and support during this research.

I want to express my gratitude to everyone who has been a part of this journey, directly or indirectly, in ways both seen and unseen. Thank you from the bottom of my heart.

ABSTRACT

Clean and sustainable energy has become the most significant necessity in the modern world due to the growth of the population and the scarcity of conventional energy sources. Moreover, using fossil fuels hurts the environment, biodiversity, and the health and well-being of both present and future generations. Currently, 30–50% of waste heat is produced by fossil fuels, and the emission of greenhouse gases and fuel consumption can be mitigated by recovering waste heat by using heat recovery techniques such as organic Rankine cycles, regenerators, and plate heat exchangers.

Thermoacoustic technology harnesses the waste heat from low-grade waste heat sources by converting it into acoustic energy and then into electricity. Still, it remains a relatively nascent field, and ongoing research is being done to develop conversion efficiency. The impact of the design parameters of the device on conversion efficiency was studied. According to the study, the working fluid temperature and the stack length are crucial to energy conversion efficiency. Based on the results, as the working fluid temperature increases, there is a noticeable rise in both pressure amplitude and volume flowrate amplitude, along with an improvement in efficiency, all while maintaining a constant regenerator length.

Similarly, efficiency increases with longer regenerator lengths when the working fluid temperature is held constant. If the working fluid temperature increases by 1 degree Celsius while maintaining the regenerator length constant, the pressure amplitude is increased by 6.2%. Higher efficiencies can be achieved by increasing the stack length, yet an upper limit exists. The efficiency is limited after a certain regenerator length because the expected acoustic behavior vanishes. These findings suggest the importance of both working fluid temperature and regenerator length in optimizing the efficiency of thermoacoustic energy conversion systems.

Keywords: Thermoacoustic, Acoustic, Travelling wave, Regenerator, DeltaEC

TABLE OF CONTENTS

LIST OF FIGURES

LIST OF TABLES

LIST OF NOMENCLATURE

γ	- specific heat ratio
δ_k	- thermal penetration depth
δ_v	- viscous penetration depth
ε_s	- correction factor for finite solid capacity
λ	- wavelength
μ	- dynamic viscosity
ρ_m	- mean density
τ	- temperature ratio
ω	- angular velocity
Δ	- difference
$\emptyset$	- porosity
a	- speed of sound
f	- frequency
f_k	- spatially averaged thermal function
f_v	- spatially averaged viscous function
k_{gas}	- thermal conductivity of gas
k_{solid}	- thermal conductivity of solid
r_h	- hydraulic radius
A	- area
A_{gas}	- cross sectional area of the gas channel
A_{solid}	- solid cross-sectional area
C	- acoustic compliance
C_p	- specific heat at constant pressure
D_{wire}	- wire diameter
H	- energy flow
I	- current
L	- inertance
P_1	- pressure amplitude
P_r	- Prandtl number
Q	- heat

Re - real component

T_c - temperature of regenerator cold face

T_h - temperature of regenerator hot face

T_m - mean temperature

U_a - velocity amplitude

U_1 - volumetric velocity amplitude

V - voltage

$\dot{W}$ - acoustic power flow

X_a - displacement amplitude

Z - acoustic impedance

CHAPTER 1

1 INTRODUCTION

1.1 Background

Clean, cost-effective, and sustainable energy has become the most significant necessity in the modern world due to the growth of the population and the scarcity of conventional energy sources. As a result, attempts to develop sustainable energy sources to meet the world's future energy needs are intensifying. According to global energy consumption trends, about 80% of total energy consumption is derived from fossil fuels. Biomass, coal, crude oil, and natural gas are used to produce electricity, transport, and perform industrial functions. The consumption of fossil fuels adversely affects the future of the world's environmental, social, and economic domains. Fossil fuels are a major source of greenhouse gas emissions, and climate change and sea level rise are the major concerns.

Moreover, air pollution, water contamination, habitat destruction, and destruction of ecosystems are also leading the world into a worse future. The continued consumption of fossil fuels leads to economic and energy crises because it is a non-renewable energy source. At present, energy recovery plays a crucial role in mitigating fossil fuel consumption by enhancing energy efficiency and maximizing the use of available energy resources. Reducing energy waste, cost savings, lowering fossil fuel demand, environmental benefits, and enhancing industrial sustainability are the reasons for the popularity of energy recovery methods.

Thermoacoustic technology combines principles of thermodynamics and acoustics to generate, amplify, or convert energy. In the modern world, thermoacoustic technology is being utilized to develop devices for power generation, refrigeration, and energy conversion. Thermoacoustic has been increasing attention and engagement due to its capacity to mitigate hazardous gas emissions, promote responsible energy consumption, efficiently harness clean energy sources, and leverage waste heat for an external power source [1]. Thermoacoustic technology has the potential to provide a sustainable and reliable solution to mitigate the consumption of fossil fuels and enhance the efficiency of energy systems by recovering the waste heat and converting it into electricity. Thermoacoustic generators (TAG) and refrigerators are two thermoacoustic devices that work based on standing or traveling acoustic waves [1].

Thermoacoustic generators (TAG), called thermoacoustic prime movers, transform thermal energy into mechanical power through a cyclic process comprising compression, heating, expansion, and cooling phases [1]. Acoustic power can be generated using only heating and cooling sources. A traveling wave is an acoustic wave that propagates without any obstructions to induce reflections along a medium filled with an infinitely long duct. A standing wave arises when the duct has a finite length, inducing reflection upon the advancing wave reaching the duct's end. The reflected wave combines with the initial wave to create constructive interference due to velocity and oscillations with magnitudes almost double that of the reference wave that propagated initially [2].

The velocity and pressure oscillations of the working fluid are nearly in the same phase alignment when the travelling wave thermoacoustic generators (TWTAGs) generating traveling waves produce acoustic waves [3]. Figure 1.1 depicts the schematic diagram of a TWTAG.

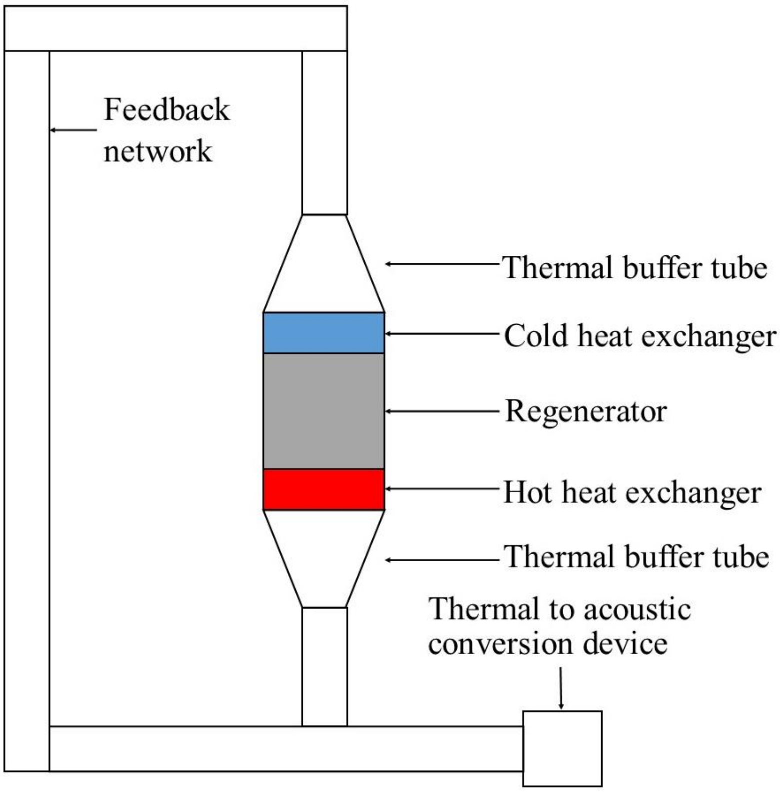

Figure 1.1 Schematic diagram of TWTAG

A regenerator constructed utilizing porous material transfers thermal energy to and from the device's working fluid, which resides between the generator's hot heat exchanger and cold heat exchangers [4]. When the working fluid parcel within the regenerator moves towards the hot heat exchanger, it undergoes a thermal expansion process. The thermal contraction process occurs when it advances towards the cold heat exchanger. The acoustic wave aids in both compression and expansion in pressure and volume due to the motion of the gas parcels within the thermal gradient established toward the cold and hot ends of the regenerator [2].

Numerous geometric configurations have been proposed for the construction of TWTAGs [5], including the multi-stage looped-tube thermoacoustic engines, single-stage looped-tube TWTAG, the torus-type engine devised by Backhaus and Swift, and the looped-tube engine with a bypass pipe, among others [6]. Transducers such as compliant audio loudspeakers, high-impedance linear alternators, piezoelectric electric generators, magnetohydrodynamic devices, electromagnetic devices, and bi-directional turbines have all been suggested for enhancing TWTAG [6].

Thermo-acoustic research began in earnest in the late 1970s and has grown dramatically in subsequent decades. In recent years, there has been a significant surge in the development of thermoacoustic refrigerators and generators. These are some of the advantages of employing TAGs [7].

- The absence of mechanical moving parts in the thermodynamic process significantly reduces the expenses associated with repairs and maintenance.
- Low initial capital investment due to simple construction utilizing common materials.
- There is much flexibility in implementation, making it easier to set up distributed energy generators.
- Flexibility and a wide temperature range
- Scalable from watts to kilowatts.

1.2 Research gap

Recent research on TAG has revealed that they can achieve thermal to acoustic conversion efficiencies ranging from around 10% to 40% depending on the design, materials, and operating conditions. The literature identifies several factors crucial for enhancing the performance of the thermoacoustic generator, including the choice of working fluid and its pressure, working fluid temperature, temperature differential between heat exchangers, design parameters of the main equipment, and optimization of load resistance. This research will employ a computational model to simulate and analyze the effects of design parameters of the regenerator and working fluid temperature on the device's performance and validate the results compared with experimental results.

1.3 Objectives of the research

- To identify the factors that affect the performance of the thermoacoustic generator.
- To identify the influence of the design parameters and operating conditions using computational modeling.
- To analyze the sensitivity of key design and operating parameters
- To fabricate the travelling wave thermoacoustic engine and experimentally validate the theoretical findings.

1.4 Methodology

Phase I

Comprehensive analysis

- Thermoacoustic phenomenon
- Computational modeling
- Case studies

Phase II

Simulating the computational

- Modelling and simulating
- Finetuning the parameters of the model

Phase III

Validation

- Fabricate a prototype
- Testing and validation

1.5 Thesis overview

This thesis consists of six chapters and their contents have been summarized as follows.

Chapter 1

The first chapter is an introduction that describes an overview of this research.

Chapter 2

The second chapter is a literature survey that describes the existing thermoacoustic technology, the core of a thermoacoustic engine, acoustic-to-electric conversion technology, and the modeling work of the thermoacoustic engine.

Chapter 3

The third chapter is the methodology, which describes how the computational model and the experimental setup were developed.

Chapter 4

The steps of the computational simulations and the conducted experiments, and their experiment setups and the results of have been mentioned in chapter four, and the chapter of discussion describes the validation of the experimental results with the computational results and the effect of the regenerator length towards the efficiency of the engine.

Chapter 5

In chapter six, the conclusion and the future works of the research have been mentioned.

CHAPTER 2

2 LITERATURE SURVEY

2.1 Introduction

After Higgins conducted the world's first experiment to demonstrate the thermoacoustic effect in 1777, the study of thermoacoustic commenced, and the experiment was named the "singing flame" [8]. Firstly, identify only the standing wave configuration; therefore, the thermoacoustic devices were of a standing wave configuration at that time. Lord Rayleigh conducted the first qualitative study on thermoacoustic in 1878. He noted that "if heat is supplied to the air during the peak of condensation or removed from it during rarefaction, it enhances the vibration" [9]. In 1969, Nikolaus Rott developed mathematical models to describe the phenomena of small amplitude oscillations within tubes, particularly focusing on scenarios involving both damping and stimulation, all while being subjected to an axial temperature gradient [8]. Rott's linear theory of thermoacoustic was the first step to analyzing the relationship between acoustic and thermodynamics. The foundation of this mathematical model rested upon the process of linearizing the equations governing continuity, momentum, and energy, thereby allowing for a systematic exploration of the dynamics inherent in the system.

P.H. Ceperley, in 1979, proposed a new thermoacoustic device that used traveling waves to generate acoustic power instead of standing waves. The efficiency of the conversion process of thermal energy to acoustic energy of this novel design was higher than the standing wave devices due to the velocity oscillations and the pressure oscillations of the system being nearly in the same phase alignment [10].

As shown in Figure 2.1, the TWTAG core comprises two heat exchangers and a porous medium called a regenerator or the stack. The hot heat exchanger (HHX) delivers the thermal energy into the system, and the excess heat is rejected by the cold heat exchanger (CHX) from the working fluid. The regenerator, located between CHX and HHX, can transfer thermal energy to or from the working fluid in the device. The thermal buffer tubes give the thermal isolation between the hot heat exchanger and the loop tube. There is a connecting tube named the feedback network, and the resonator is situated at the end of the feedback network [11]. The acoustic-to-electric conversion device is connected to the resonator to conversion process [12].

Figure 2.1 also illustrates how to generate acoustic waves inside the TWTAG's core. A gas parcel near the heat exchanger at a low temperature rejects the heat and then compresses the parcel by reducing its volume. Then, it goes towards the hot heat exchanger, where the heat is absorbed, and its temperature increases. Then, the gas parcel is expanded due to temperature increments. After the expansion process, the gas parcel returns to the cold heat exchanger and undergoes this process repeatedly. Due to this process, the acoustic waves are generated inside the core and propagate through the feedback network.

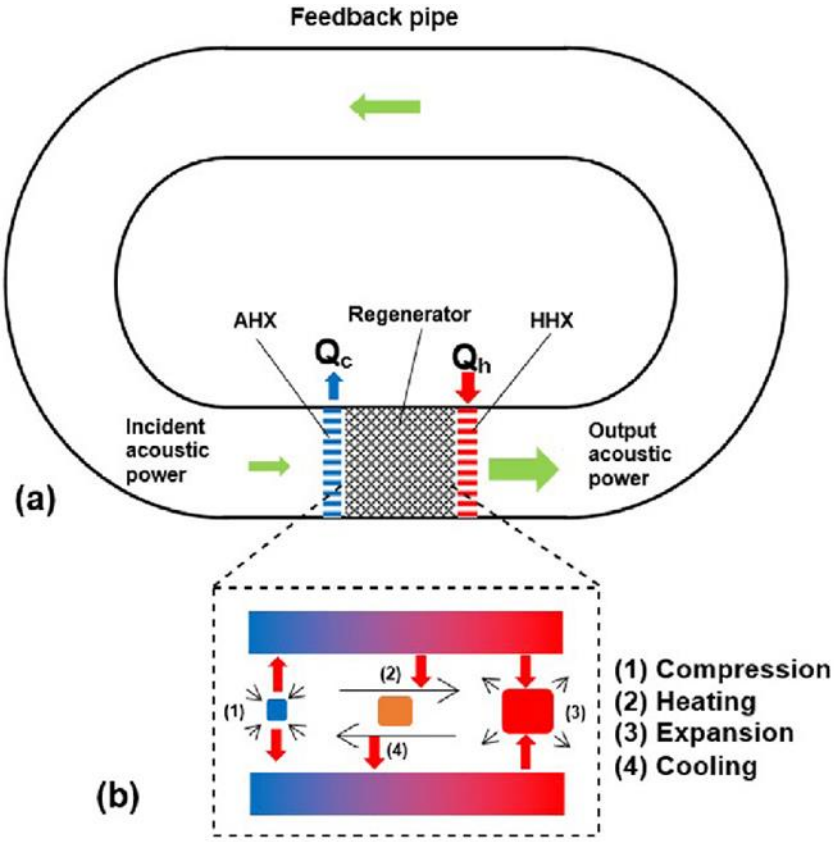

Figure 2.1 (a) - Components of thermoacoustic core (b) - Movements of gas parcel in the regenerator. Adapted from [23]

After introducing the traveling wave concept, many research programs were conducted to develop thermoacoustic device properties and efficiency. In that case, the Los Alamos National Laboratory in the Netherlands did a great job of developing that concept, and they did much research that improved the efficiency of the thermoacoustic devices by employing techniques aimed at minimizing the effects of viscous flow losses and heat streaming [13]. Furthermore, a group of researchers from the Los Alamos National Laboratory worked together to implement a sophisticated computer program designed specifically for simulating the behavior of thermoacoustic systems. It was named Design Environment for Low-Amplitude Thermoacoustic Energy Conversion (DeltaEC). After this was launched, researchers could predict or model the thermoacoustic devices before it manufactured. The DeltaEC software, renowned for its advanced capabilities, can forecast various key parameters, including acoustic power, acoustic pressure, temperature, volumetric efficiency, and overall power output of the thermoacoustic device, offering a comprehensive analysis of its performance characteristics [13].

2.2 Acoustic core (Heat exchangers and regenerator)

The central operational element of a thermoacoustic device predominantly comprises a regenerator intricately situated between a hot heat exchanger and a cold heat exchanger, enabling the efficient transfer of thermal energy within the system. A thermoacoustic engine's driving force is the regenerator, a porous medium possessing the capacity for efficient heat exchange with the working fluid in the device strategically positioned between regions of low and high-temperature gradients within the system. Due to the temperature difference of the two heat exchangers, a substantial temperature gradient is established along the regenerator length axially [14], [15]

A parcel of gas is heated when it is moved toward the hot heat exchanger and cooled when it is displaced toward the cold heat exchanger due to the cyclic motion of the acoustic wave [16]. As the working fluid experiences oscillations, the regenerator operates similarly to a series of thin heat exchangers. Within the thermal gradient established through the regenerator of TWTAG, the acoustic wave triggers compression, expansion, and displacement towards both heat exchangers, thus enabling the effective transfer of thermal energy [2]. The efficiency of the thermoacoustic engine primarily hinges on regenerator performance [15]. In the fabricating phase of a TWTAG, it is imperative to conduct testing by systematically varying parameters such as regenerator length, mesh size, and mesh material, as these factors significantly influence its operational effectiveness.

The performance of TWTAG can be enhanced by adjusting the length and porosity of heat exchangers. Brewster and the team did the numerical simulations, and according to their findings, the geometry of the heat exchanger is a very important factor for efficient heat transfer between the working fluid and the solid. The major mode of heat transfer in the thermoacoustic core is convection, and the acoustic oscillations of the working fluid develop it [17]. Also, in the parallel-plate heat exchanger, the plate spacing is a major factor that can be affected by the heat transfer rate and efficiency. Moreover, with the increment of the heat exchanger length and the device's operating frequency, the heat exchanger's effectiveness is decreased [18]. An optimal length for the heat exchangers can be identified by relying on factors such as plate spacing, plate thickness, amplitude of the acoustic wave, and the Reynolds number of the working fluid [19]. The porosity of both heat exchangers should be higher to enhance the efficiency, acoustic power, and pressure amplitude of the TWTAGs. When the porosity is high, the shorter CHX performs better, while the longer HHX improves the system's efficiency [20].

Ahmed Hamood and the team researched developing a two-stage TWTAG. They aimed to convert waste heat from internal combustion engine (IC engine) exhaust gases via the thermoacoustic device into electric power[21]. The experimental setup contains two identical powering stages of the system, all of which have an acoustic energy harvesting device and a linear alternator coupled with these components at harvesting points. The acoustic waves in identical stages have similar volumes and pressure flow rate amplitudes. However, between the two stages, there is a 180-degree phase angle. Consequently, one stage exerts a pushing force.

Meanwhile, the interaction of these out-of-phase acoustic fields with the alternator exerts a pulling force on the piston [21]. The thermoacoustic generator features a looped tube configuration extending over a length of 16.1 m, accommodating a TWTAG that has two stages operating on Helium gas pressure at 28 bar is utilized as the operating medium of the device and functioning at a constant frequency of 54.7 Hz. The traveling wave thermoacoustic implements strategic design measures for harvesting acoustic energy. To address potential gas leakage concerns at high-temperature conditions within the sealant of high-temperature components, the thermal buffer tube, hot heat exchanger, and regenerator holder have been integrated into a single unit. Additionally, the regenerators are strategically positioned near regions experiencing minimum volumetric velocity amplitudes and maximum pressure amplitudes of gas parcels, aligning with the system's highest acoustic impedance to minimize the system's viscous dissipation [21].

Wigdan Kisha and Paul Riley did their research through the asymmetrically heated multistage thermoacoustic generator. According to their research, the unbalanced acoustic impedance in the engine was managed effectively to increase the efficiency of the thermoacoustic generator. With this novel method, both computational and experimental results demonstrate an increase in loop acoustic power. According to the findings from the DeltaEC code, when the heat supplied into the system shifted from a balanced 50%:50% ratio to a 40%:60% ratio, the acoustic power output of the system generated by the acoustic core increased gradually from 24.4 W to 31.4 W. According to the computational model results, the optimal ratio given maximum electric power output was 30%:60% [22]. Moreover, it was observed that not only did the onset temperature of the thermoacoustic engine decrease along the asymmetrical temperature ratio but it was also noted to be 40°C at the optimal ratio [2].

Artur J. Jaworski and O.A. Abdoulla-Latiwish collaborated to develop a TWTAG consisting of two waste heat storage stages. The 94 layers of stainless-steel rectangular mesh screens are utilized for constructing the generator (stack) integrated into the regenerator of the thermoacoustic engine. The number 34 was used as the mesh number and 0.16mm was the diameter of a wire of the mesh [23]. After the calculations, the porosity and the hydraulic radius values are 83.3μm and 198μm, respectively. This paper proposes a minor modification, suggesting the adoption of "flattened tubes." These tubes offer channels with high aspect ratios, diminishing their hydraulic radius. During this study, the area that can transfer heat between the working fluid and the flue gas and the porosity of the hot heat exchanger were developed and increased [23].

Honghao Pan, Daming Sun, and Jie Zhang collaborated to develop a TWTAG consisting of three identical stages, which was later analyzed using DeltaEC software. According to their findings, the regenerator's length and porosity directly influenced the engine's efficiency. The ultimate power output was gained with the 0.9 porosity level, and generally, the higher porosity level leads to lower viscosity losses inside the regenerator [24]. When the thermal penetration depth closely matches the hydraulic radius of the device, the maximum results were attained. However, the most efficient heat transfer performance was observed at approximately one-third of the thermal penetration depth [23], [24].

2.3 Piping network and working fluid

In TWTAGs, the onset of the traveling waves in the device happens in the loop of pipes connected into thermal buffer tubes to both cold and hot heat exchangers, with an acoustic loop with a discontinuous acoustic path. This feedback mechanism is represented through a model resembling a fundamental waveguide, incorporating characteristics such as inertia, compliance, and resistance [2].

In TWTAGs comprising an odd number of stages, incorporating a small stub resonator made out of PVC with a terminating end becomes necessary. The stub of TWTAGs offers the supplementary volume required to initiate oscillations in the device, apart from that the stub can be likened to a lumped capacitance component. Ideally, the stub resonator is designed to match the area of the resonator's length, and the feedback loop's cross-section should be nearly equal to one-tenth of the wavelength [2]. The operational frequency of the TWTAG tends to vary depending on the length of the acoustic piping network. The loop's length should correspond with the wavelength to achieve optimal propagation of the traveling acoustic wave. The acoustic loop should typically feature smooth surfaces, gentle bends, and a uniform cross-sectional area to minimize acoustic losses [2],[25].

The performance of the thermoacoustic engine is directly influenced by the properties of the working fluid and the mean pressure. Specifically, high mean pressure and speed of sound within the engine are crucial for achieving optimal performance [26]. Also, light gases improve the engine's efficiency because of their high thermal characteristics and high speed of sound. By the way, air in atmospheric conditions can be used as the working fluid, reducing the cost and complexity of the component [25].

Reducing the viscous penetration depth and increasing the thermal penetration depth of the working fluid are key factors in enhancing the efficiency of the TWTAG [27]. Lowering the viscous penetration depth improves the engine's efficiency while increasing the thermal penetration depth correlates with an increase in the TWTAG's efficiency [27]. Increasing the thermal penetration depth enhances thermal contact with the working fluid. Considering these factors, Carbon dioxide, Nitrogen, and Helium have been employed as working fluids in TWTAG to enhance efficiency. As heating power increases, pressure ratio and temperature rise among these gases.

Additionally, mean pressure escalates with an increment of pressure ratio and heating temperature [27]. Carbon dioxide has the smallest onset temperature, and it could be given better performance for low-grade heat engines. Helium has the lowest heating temperature and the highest oscillating pressure amplitude, considering the above three gases. Therefore, helium gives the highest efficiency of the TWTAG. The heat is transferred more efficiently with the regenerator by the helium because it has the highest thermal penetration depth considering the above three gases [5].

Artur J. Jaworski and O.A. Abdoulla-Latiwish investigated the impact of stub length on engine efficiency. Their findings revealed that the maximum efficiency and engine power output were achieved with a stub length of 1090 mm [23]. The engine's power and efficiency decreased with the length of the system's stub tube. Moreover, the constrained displacement of the diaphragm during tests significantly affects the alignment already observed and estimated total efficiency with the optimal length of the stub tube. This effect becomes more pronounced when the acoustic velocity amplitudes of the system are large. As a result, the alternator coil's vibrations exceeded the magnetic gap. Moreover, the corresponding escalation in detrimental acoustic streaming of the system was increased due to the increment of the stub tube length [23].

2.4 Acoustic to electric power conversion

For harvesting power from the engine, a device is necessary that is capable of converting the acoustic energy into electric energy generated by the TWTAG. Researchers have explored various methods to meet this requirement. The following is a list of devices utilized in the conversion process [28]. The classification of conversion type is shown in Figure 2.2 below.

- Piezoelectric generators
- Magnetohydrodynamic devices
- Electromagnetic devices
- Bi-directional turbines.

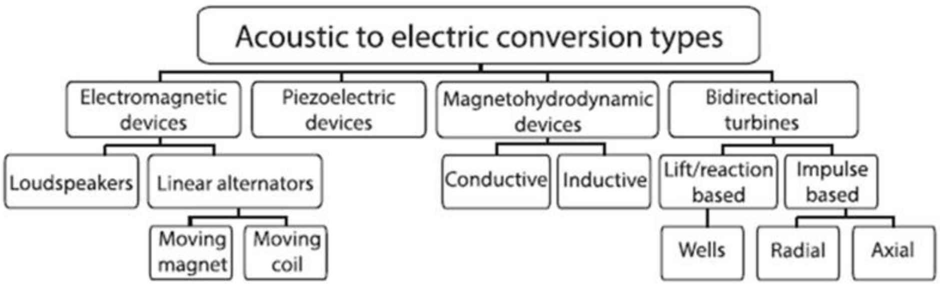

Figure 2.2 Classification of acoustic to electric conversion devices. Adapted from [28]

The electromagnetic category will include instruments that convert acoustic and electrical power via electromagnetic induction. Iron is usually included for cheaper costs and greater transduction efficiency, in addition to magnets and coils, which are essential components for electromagnetic induction; the fundamental concept of these devices involves utilizing acoustic power to induce mechanical displacements in one stationary part of the device relative to the other moving two, thereby generating a small amount of electric power in the alternator's copper coil. Various arrangements can be implemented to ensure relative mobility [28].

Conventional loudspeakers are used for generating sound using electricity. In this manner, the loudspeakers are used in the reverse direction; sound waves produce the force on the cone to oscillate in the axial direction and induce an electric current; one approach involves moving the interconnected coil about the permanent magnets. Many of the research used the loudspeaker as the conversion device because they were very cheap and readily available [28]. The schematic diagram of a conventional loudspeaker is shown in Figure 2.3. When a loudspeaker is used as the conversion device, the operating frequency should be chosen according to the characteristics of the loudspeaker [25]. Most of the time loudspeakers were used with low power, low frequency (50-100 Hz) TWTAGs. Therefore, their paper cones are weak and brittle, with short stroke lengths and low impedance [28].

Linear alternators can be used as a conversion device instead of the loudspeaker. The efficiency of the conversion process of the linear alternators is higher than the conventional loudspeakers. Two main types of linear alternators can be used in TWTAGs: moving coil type and moving magnet type. The linear alternators were provided with 1 kW of power output with 75% efficiency in converting acoustic power into electric power within the system [28].

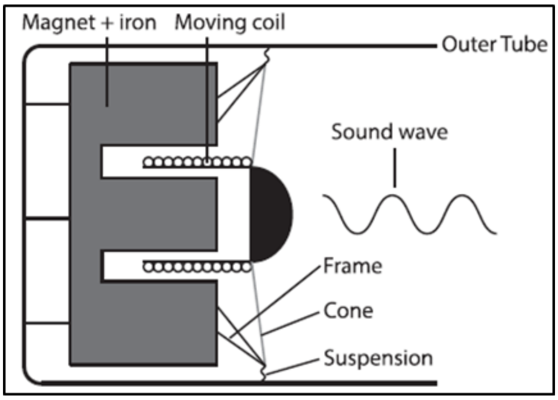

Figure 2.3 Schematic diagram of loudspeaker. Adapted from [28]

Abdoulla-Latiwish and Artur J. Jaworski developed a two-stage TWTAG driven using waste heat to generate electricity in developing countries. A commercially available loudspeaker was utilized as the linear alternator. The prototype generates 14.2W of electrical power when connected to a 9 Ω load, with a stub tube length of 1070mm [23]. The loudspeaker was enclosed within the stub tube using a short connecting tube as a separate branch. To achieve low acoustic impedance and high acoustic dissipation, 2-inch diameter PVC pipes were used in the system. The prototype attained a thermal-to-electric efficiency of 2.1%. The efficiency of the system can potentially be increased by improving the heat exchange process of the heat exchangers [23].

T. Biwa, G. Penelet, and T. Watanabe developed a moving piston frictionless sterling engine featuring solely a piston assembly attached to a flywheel. The conversion process of the reciprocating motion into the rotational motion is done by the power piston attached to the flywheel shown in Figure 2.4. Due to this circular motion, a conventional alternator can be employed instead of a linear alternator, which is more readily available [29]. The engine utilized a connecting rod made of aluminum, a flywheel made of brass, and a piston assembly with a glass cylinder. The piston's top dead center was positioned level with the top of the piston cylinder and the diameter of the piston and length of 35 mm and 158 mm, respectivel [29].

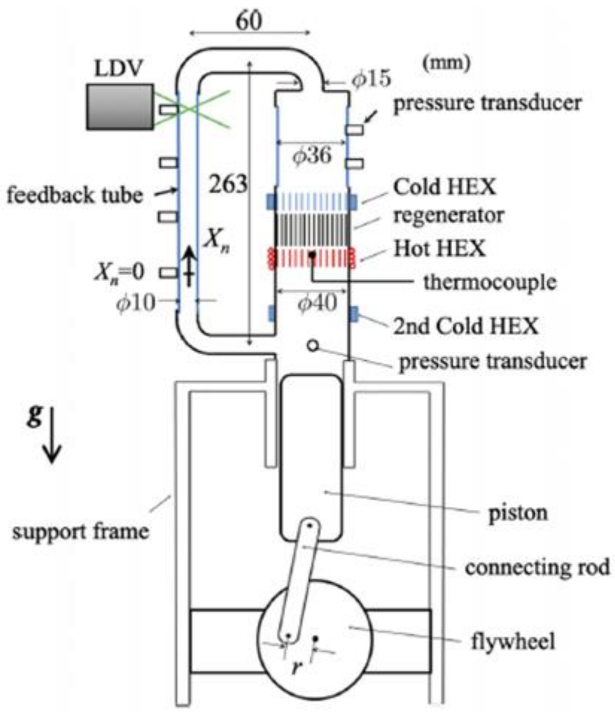

Figure 2.4 Flywheel-based TWTAG. Adapted from [29]

2.5 Modeling work

DeltaEC can serve as a predictive tool for the performance of thermoacoustic devices or assist in designing equipment to attain specific objectives. Researchers in physical acoustics, especially those focused on thermoacoustic studies and experiments, will find DeltaEC advantageous for their investigations.

DeltaEC utilizes numerical integration of a one-dimensional wave equation within a user-specified liquid or gas medium and geometry. It can manage configurations such as complete thermoacoustic engines, electro-acoustically powered freezers, resonators, duct networks, and thermoacoustic mixture separators. Additionally, DeltaEC can accommodate specific acoustic components and complex geometric designs smartly [30]. A DeltaEC model constructs a system of nonlinear equations from the model based on the user-selected initial targets and guesses. It then iteratively adjusts the user's initial guesses to ensure that the integration results align with the specified user-selected targets [13].

DeltaEC ensures continuity of velocity (U_1) and pressure (P_1) as it transitions from the edge of one segment to the start of the subsequent segment. The propagation of the wave in the model within each segment is influenced by local characteristics like length permitter and size, along with its global parameters, such as acoustic frequency. For simpler segment problems, DeltaEC uses analytical solutions to the governing equations, but it relies on numerical methods to achieve solutions for more complex scenarios [13].

DeltaEC utilizes basic segments in modeling work such as HX, Hardend, TX, Stkrect, Surface, Duct, and RPN. Other minor segments may also be necessary to accurately define the system and achieve precise simulation results [13]. In a DeltaEC model, natural inputs include the dimensions of each part specified by segments, initial values for velocity, mean temperature (T_m), and pressure at the start of the segment list, as well as energy inputs from HHX and CHX or the power supply to the transducers. The model also provided Several natural outputs, including a forecast of temperature variation through the regenerator of the thermoacoustic engine, energy flows throughout the device, T_m, U_1, and P_1 of the thermoacoustic engine [3].

In the DeltaEC model, the number of natural inputs and the number of natural outputs the user specified are the same. Also, the model can iteratively adjust those guesses and targets during analytical calculations. This capability of DeltaEC effectively allows for swapping natural inputs with outputs and vice versa, optimizing the DeltaEC model to achieve the desired outcomes smartly [3].

Utilizing available data in the literature, the modeling and validation process of a single-stage TWTAG was done [31]. The maximum efficiency of the engine was forecasted by utilizing the validated model under optimal conditions. According to the findings, the system's efficiency could be enhanced by increasing the temperature of the hot heat exchanger. According to the results, the system's frequency increases linearly within the range of ambient temperatures considered for the study. Also, it was observed that the frequency remains relatively constant when varying the pressure within the considered range, showing no significant changes [31].

CHAPTER 3

3 METHODOLOGY

3.1 Mathematical Modeling

Before getting into the details of the design for a thermoacoustic system, several thermal and acoustic principles must be discussed. The field of thermoacoustic consists of theories of thermodynamics as well as acoustics. Two main types of configurations are utilized in thermoacoustic technology to design and analyze them. They are named standing wave and traveling wave devices.

The sound waves require a medium to propagate from one location to another location by generating compression and refraction regions within the medium within which the particles vibrate back and forth. As a result of the vibrations of the particles, the pressure and the velocity oscillations are generated when an acoustic wave propagates through the medium. Also, the medium's temperature and density oscillate with the acoustic wave. The acoustic waves generated in the thermoacoustic devices are considered one-dimensional waves [32]. They propagate only along the length of the device longitudinally. Furthermore, the lateral dimensions of the devices are designed such that they are smaller than the wavelength of the acoustic wave that is generated within the device [2]. When an acoustic wave propagates within the thermoacoustic device, if the duct has a finite length, at the end of the duct, the propagating wave is reflected due to the obstacle. Then the wave generated through the reflection interferes with the original wave, and a standing wave is generated within the system. The waves propagating through the duct which has an infinite length without any obstacles are called travelling waves.

The relation between the frequency (f), wavelength (λ), and speed of the sound (a) is defined by equation 3.1. Where the ω is the angular velocity.

$$a = f\lambda = \frac{\omega\lambda}{2\pi} \tag{3.1}$$

The wavelength of the acoustic wave propagating in the thermoacoustic device is determined by the length of the duct and its end conditions. When the device's duct is both ends closed or opened with a bounded length, two times the duct length of the device is equal to the wavelength. When it has a finite length and also it is an unending looped duct, the length of the duct matches the acoustic wavelength [32], [33].

In thermoacoustic generators, thermal energy is transformed into acoustic energy. Later, the acoustic energy is converted into electricity by utilizing an acoustic-to-electric conversion device [33]. According to the literature, there are two types of thermoacoustic devices that can convert thermal energy into acoustic according to their operation principle. The traveling wave devices are more efficient than the standing wave devices due to the velocity oscillations and are almost pressure variations perfectly same phase [34]. The heating and cooling processes are taken by the heat exchangers and the porous medium named regenerator is provided the power amplification facility based on the Stirling-like thermodynamic cycle in the thermoacoustic device's core [2]. The gas parcels between hot and cold heat exchangers experience thermal contractions and expansions. Due to these displacements, the pressure and the volume of the working fluid inside the device are oscillated, and an acoustic wave is generated through the device. The temperature gradient between the hot and cold heat exchangers is the driving force of the acoustic wave generated within the system [35].

The thermal energy generated within a unit time by the two heat cartridges (Q_h) was calculated using the equation 3.2 given below. Where the *V* is the voltage across the heaters, and *I* is the current flowing through the heaters.

$$\dot{Q}_h = VI \tag{3.2}$$

The thermal energy absorbed by the cooling water at the CHX is given by equation 3.3 where the C_p is the specific heat capacity of water, ρ_w is the density of the water and U_w is the volume flowrate of the water through the CHX. The temperature of cooling water at the outlet and inlet of CHX are represented by T_{in} and T_{out}.

$$\dot{Q}_w = \rho_w c_p U_w (T_{out} - T_{in}) \tag{3.3}$$

The acoustic power ($\dot{W}$) of the system is given by equation 3.4 and the two-sensor method was used [34].

$$\dot{W} = \frac{A}{2\omega\rho_m \Delta x} |P_{1A}||P_{1B}| \sin\theta \tag{3.4}$$

The thermoacoustic phenomenon is mathematically modeled by considering an acoustic wave propagating through the medium and its energy transfer with the medium [2]. The energy and the wave equations for an acoustic wave propagating through a compressible fluid were derived by Rott [36]. Starting from Rott's acoustic approximations, three main equations were derived to calculate the key outcomes of the thermoacoustic engines. Two homogeneous wave equations were derived to analyze the momentum (3.5) and the continuity (3.6) of the flow, and the other equation was derived for analyzing the energy (3.7) flow due to the interaction between acoustic and temperature fields [31], [37]. The mean values and first-order fluctuations are denoted by subscripts m and 1, and the tilde "~" stands for the complex conjugate.

$$\frac{dp_1}{dx} = -\frac{i\omega\rho_m}{(1 - f_v)A_{gas}} U_1 \tag{3.5}$$

$$\frac{dU_1}{dx} = \frac{i\omega A_{gas}}{\rho_m a^2}\left(1 + \frac{(\gamma - 1)f_k}{1 + \varepsilon_s}\right)p_1 + \frac{f_k - f_v}{(1 - Pr)(1 - f_v)(1 + \varepsilon_s)} \frac{U_1 dT_m}{T_m dx} \tag{3.6}$$

$$H = \frac{1}{2} Re \left[p_1 \widetilde{U}_1 (1 - \frac{f_k - \tilde{f}_v}{(1 + \varepsilon_s)(1 + Pr)\left(1 - \tilde{f}_v\right)} \right]$$

$$+ \frac{p_m c_{p,m} |U_1|^2}{2A_{gas} \omega (1 - Pr|1 - f_v|^2)} \frac{dT_m}{dx} Im$$

$$\times \left[f_k + \frac{(f_k - \tilde{f}_v)(1 + \varepsilon_s f_v / f_k}{(1 + \varepsilon_s)(1 + Pr)} \right]$$

$$- \left(A_{gas} K_{gas} + A_{solid} K_{solid} \right) \frac{dT_m}{dx} \quad (3.7)$$

The regenerator consists of a network of parallel channels filled with a working fluid with varying inertance, compliance, and resistance. The compliance (C) or the compressibility of the working fluid in a channel volume can be calculated using equation 3.8, and the inertance (L) of the working fluid in the same channel is in equation 3.9.

$$C = \frac{v}{\gamma p_m} \quad (3.8)$$

$$L = \frac{\rho_m \Delta x}{A} \quad (3.9)$$

When the temperature is changed along with the regenerator, the density of the working fluid should be changed inversely proportionally. Furthermore, the volumetric velocity of the gas parcels should be increased proportionally [2].

3.2 Computational Implementation

Evaluation of expected design changes can be done quickly and affordably with computer simulations. Above mentioned principles in linear thermoacoustic are applied with additional complex effects in more complex thermoacoustic systems that can be modeled utilizing computational tools. The Design Environment for Low Amplitude Thermoacoustic Energy Conversion (DeltaEC) is one of the computer programs that was developed by the research group of the Los Alamos National Laboratory to use model thermoacoustic devices. By matching the volumetric flow rates, pressure, and temperature of the junctions of segments that the user defined, the linear thermoacoustic equations are numerically integrated by the DeltaEC on one dimension [13]. DeltaEC uses sinusoidal time dependence with a low-amplitude acoustic approximation to integrate in one spatial dimension numerically. It incorporates the wave equation and occasionally additional equations, including the energy equation, in a gas using the user's specified geometry as a series of segments, including ducts, compliances, transducers, thermoacoustic stacks, and regenerators [32]. DeltaEC can forecast how a TWTAG operates, or it gives ideas to the designer to fabricate equipment to obtain the required results. Researchers in physical acoustics, particularly thermoacoustic, will benefit from DeltaEC.

The first simulated model had been validated with the experimental results and Mitchell McGaughy developed it during his master’s [2]. The DeltaEC model consists of a hot heat exchanger (HHX), a cold heat exchanger (CHX), a regenerator, thermal buffer tubes (TBT), an acoustic feedback piping network, and a stub. According to the design, the segments we want to add to the model can easily be added using the insert command. If we want to expand the model, we can expand the entire model or the required segment.

After running the simulation, completing the program and the calculations takes several minutes. The time taken to do the calculations depends on the computational power of the processor of the computer. After successfully running, it gives us the green light and possible outcomes according to the input values, guesses, and target values. The values you want to find using the model should be the guesses, and the values you will consider as knowns should be the targets. The number of targets and the guesses should be equal [13].

The model that was developed by McGaughy consists of a cold heat exchanger fabricated using a shell and tube, and a parallel plate is used to fabricate HHX. The regenerator of the system was modeled as a stack of mesh screens made out of stainless steel. The model's acoustic core is almost double the cross-sectional size of the feedback network. The feedback network pipe was designed with a constant cross-section to minimize dissipative effects. The modeling process was started in the middle of the feedback network, and the segments were gradually added to the model towards the cols heat exchanger. Under different temperature conditions, the simulations were performed.

A new model was developed according to the dimensions of the proposed experimental setup to analyze the performance. All the dimensions of the segments in the model had to be changed according to the experimental setup, and the two shell and tube-type heat exchangers were used as the model's cold and hot heat exchangers. The operational parameters of the new model are shown in Table 3.1 below.

Table 3.1 Operational parameters of the new model

Parameter	Value
Mean temperature	320 K
Mean pressure	1.0133E+05 Pa
Pressure amplitude	821.93 Pa
Volume flowrate amplitude	4.2567E-03 m^3/s
Total length	5.96 m
Operational frequency	58 Hz

Figure 3.1 below depicts the interface of the model developed during the study. The main segments and their dimensions are given in Table 3.2 below. The values were selected based on the literature, availability, and cost.

Table 3.2 Dimensions of main segments of new model

Segment	Dimensions in mm
Regenerator	Length – 15 to 30
	Diameter - 83
HHX	Length - 20
	Diameter - 83
CHX	Length - 20
	Diameter - 83
Feedback network	Length - 5960
	Diameter - 63

Another approach of the test was the impact of the diameter of the regenerator of the thermoacoustic generator on the volume flow rate amplitude, pressure amplitude, thermal input at HHX, and the device's efficiency were numerically analyzed. The pressure amplitude and the volume flowrate amplitude of the oscillations, heat input at the HHX, and the efficiency of TWTAG were analyzed by altering the diameter of the regenerator. The diameters of the hot heat exchanger and the cold heat exchanger were also arranged with the diameter of the regenerator to continue the acoustic waves inside the engine without any losses or changing their length. Including the lengths of the heat exchangers and the regenerator, the total length of the device used to analyze is 5.4 m. There was no change in the length of the main segments with the existing model. The temperature of the HHX was kept constant at 1110K during the simulations. Ambient air at pressure 101.325 kPa was utilized as the working fluid of the device, with the frequency assumed to be 54 Hz. In this study, the regenerator diameter increased from 0.1 m to 0.18 m with a 0.005 m increment. The diameter range of the regenerator was selected based on the experimental setup that is being developed and the literature.

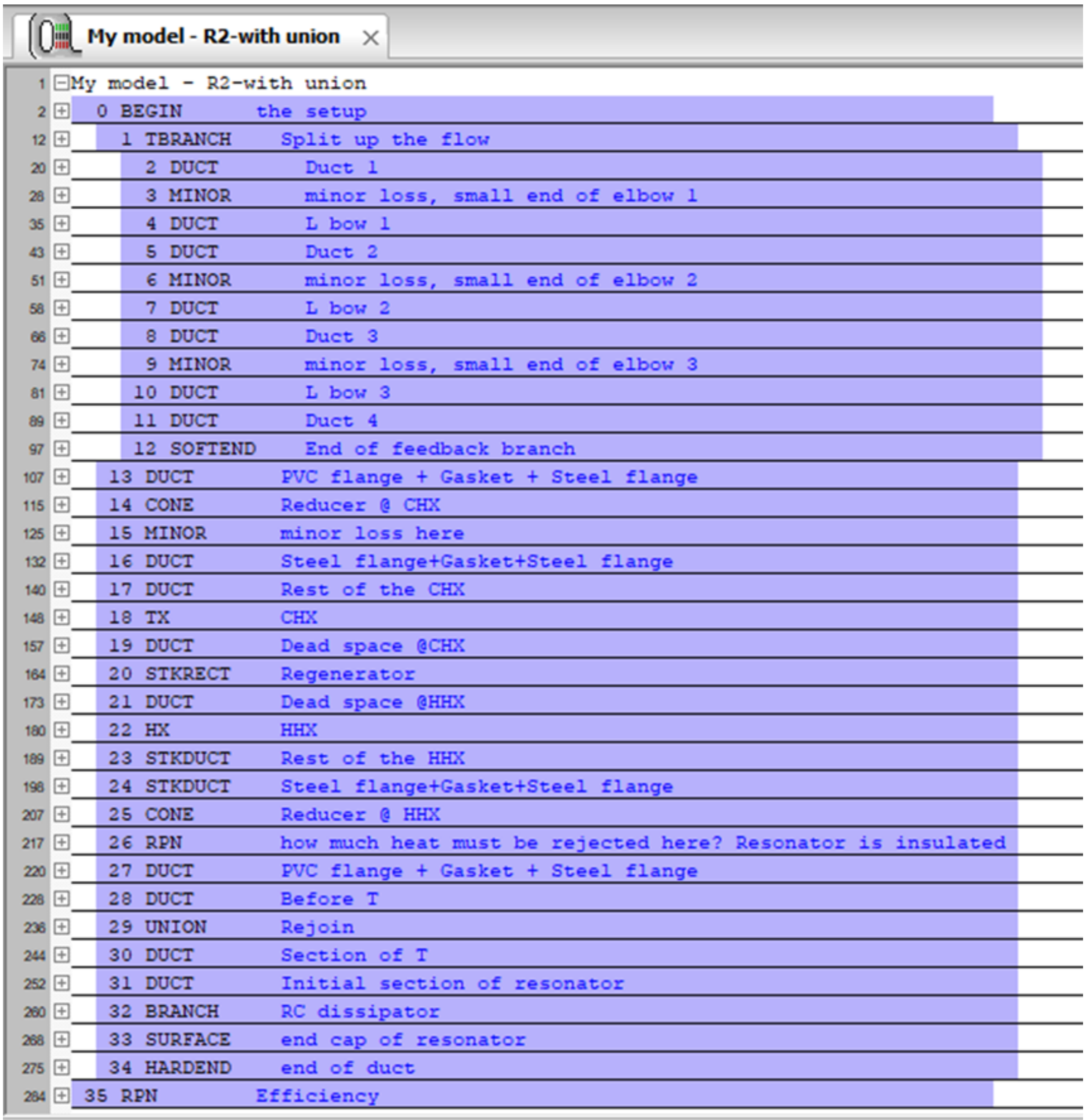

Figure 3.1 Interface of the new model

3.3 CFD Modeling

Computational Fluid Dynamics (CFD) modeling is used in the modern designing process to analyze the fluid flow pattern and heat transfer and to reduce the cost of physical prototyping. Moreover, it supports exploring innovative designs considering the various types of materials and unconventional geometries while saving cost and time. During the study, CFD modeling was used to analyze the heat exchangers of the thermoacoustic core. The 3D model of the heat exchanger that was designed is shown in Figure 3.2 below. There are two holes through the heat exchanger for inserting the cartridge-type heaters, and it is the thermal source. The gap between the two heaters was changed during the simulation from 17mm to 20 mm and given 460W constant heat flux through the wall of the above-mentioned holes. The maximum reachable temperature and the temperature distribution were compared to selecting the best design from them.

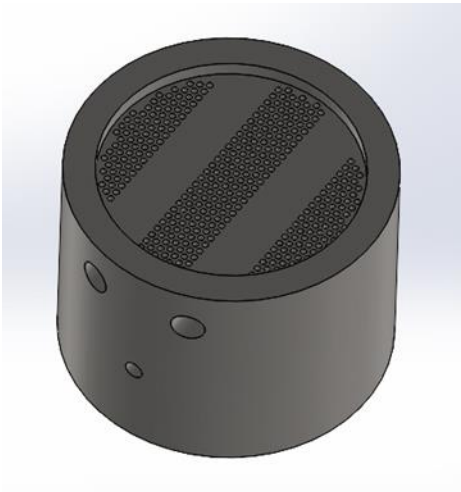

Figure 3.2 model of the heat exchanger

3.4 Experimental Apparatus

The design and fabrication of the thermoacoustic device were very challenging because it dealt with sensitive operational parameters such as pressure and temperature. The fabrication facilities, manufacturing methods, cost, and performance characteristics were the main factors that had to be considered during the design process of the thermoacoustic device. Initially, a 3D model was developed based on the dimensions extracted from the calculations, simulations, and the relevant literature sources considering manufacturability, availability, and cost.

3.4.1 Operational parameters

The working fluid is the main factor that can affect the performance of a thermoacoustic engine. The acoustic wave that is generated in the core is propagated through the working fluid within the device, from the acoustic core to the acoustic to the electricity conversion device. Therefore, the working fluid should have high thermal conductivity characteristics and a high speed of sound. Due to these reasons, the light gases are more suitable as the working fluid [38]. There is a tendency to use inert gases as the working fluid in most of the research. In this research, atmospheric air is used as the working fluid due to its availability and cost-effectiveness, and the complexity of component design has also been reduced.

It was crucial to finalize several length scales of segments in the designing and fabricating process of TWTAG. The thermal penetration depth, gas displacement amplitude, and viscous penetration depth were key parameters to ensure the efficient energy transfer process within the system. The ratio between the acoustic velocity to acoustic frequency is defined as the gas displacement amplitude (Xa) of the wave that propagates along the direction of the device. It is given by equation 3.10.

$$X_a = \frac{u_a}{\omega} \tag{3.10}$$

Along with the lateral direction of the device, the viscous penetration depth and thermal penetration depth were considered due to their importance towards the properties of heat and viscous. Equation 3.11 defines the thermal penetration depth (δ_k) as the distance a thermal wave penetrates into a material over a given time, influenced by the thermal diffusivity of the material and occurring laterally during acoustic oscillations.

$$\delta_k = \sqrt{\frac{2k}{\omega \rho C_p}} \tag{3.11}$$

The viscous penetration depth (δ_v) given in equation 3.12 refers to the distance that momentum can be transferred along the lateral direction within the system due to the solid boundary oscillating or when there is a time-varying flow near the boundary.

$$\delta_v = \sqrt{\frac{2\mu}{\omega\rho}} \tag{3.12}$$

The operating frequency of the device should be matched with the resonant frequency of the device, which is going to be used to convert acoustic energy into electricity to harness acoustic energy at maximum [35].

3.4.2 Thermoacoustic core

The thermoacoustic core consists of a regenerator, a hot heat exchanger, and a cold heat exchanger. The main objective of a heat exchanger used in TWTAG is to facilitate efficient interaction between heat and the working fluid while minimizing the destruction of acoustic energy [35]. Generally, the length of heat exchangers of thermoacoustic devices corresponds to two times the displacement amplitude of the gas. Heat exchangers exceeding this length experience unnecessary acoustic dissipation, compromising heat transfer efficiency [2]. As a result of changing the diameter of the thermoacoustic core in relation to the device's feedback network, it is possible to decrease the velocity within the core. This adjustment increases impedance in the acoustic core, effectively minimizing losses in converting thermal into acoustic energy. Additionally, the thermoacoustic core with a considerable size cross-section presents the potential for enhanced transfer of heat energy between the working fluid and the heat exchangers. Normally, the diameter of the core is greater than the diameter of the feedback pipes. According to the literature, the optimum outcomes are delivered by the thermoacoustic cores which have two to three times higher cross-sectional areas concerning the cross-section of the feedback network pipes [39].

Multiple factors, such as the design of the components, manufacturing process, performance attributes, and cost considerations, influence the heat exchanger material selection. For applications involving low temperatures, copper is favored as the material used for heat exchanger fabrications. The reason is the heat transfer coefficient is high despite the cost of the materials. Alternatively, aluminum presents a cost-effective substitute for copper, offering advantageous thermal properties and ease of machining. Stainless steel, while typically regarded as having lower thermal conductivity, is notable for its high maximum service temperature limits and cost-effectiveness [39].

The fabricated hot heat exchanger depicted in Figure 3.3 is made of mild steel. It has an 83 mm diameter, 20mm thickness, and 2mm holes through it.

During the fabrication process of HHX and CHX, a 3-axis CNC milling center was used to mill the material. At the end of the 3D modeling process, the G code of the milling process was generated using CAD software and then fed into the milling center. The manufacturing process step is shown in Figure 3.4, given below.

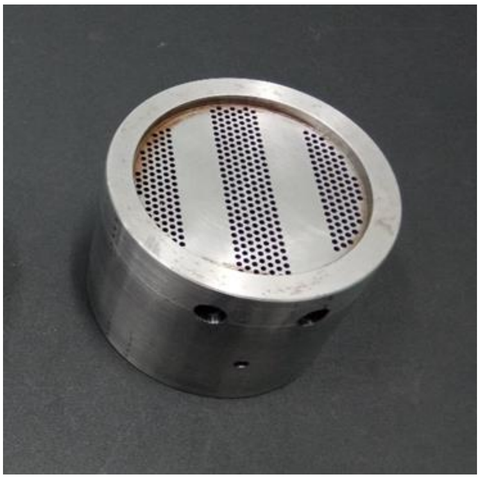

Figure 3.3 Fabricated hot heat exchanger

Figure 3.4 Steps of the manufacturing process of HHX and CHX

The hot heat exchanger is fitted with two heating cartridges, each operating at 230 V and each measuring 10 mm in diameter and length of 60 mm, illustrated in Figure 4.5. These heat cartridges have the capacity to generate heat up to 230 W while maintaining the operating temperature at a maximum of 600K. While the heat exchanger has the capability to produce thermal energy at the total rate of 460 W, the upper limit of heat supply is constrained by the maximum operating temperature of the heaters. To monitor and prevent overheating conditions, a K-type thermocouple is attached to the heat exchanger, as shown in Figure 3.5, which is utilized to track the temperature of the surface of a designated cartridge-type heater.

The configuration of the CHX closely mirrors that of the HHX, as shown in Figure 3.6. However, it incorporates a water jacket surrounding the heat exchanger to facilitate temperature control. This is achieved by circulating water through the jacket, ensuring the maintenance of desired temperature levels. A K-type thermocouple was attached to the CHX to take the temperature readings of CHX, and another two K-type thermocouples were attached to the water inlet and water outlet of the CHX.

The component named regenerator, functioning as a porous medium, engages in exchanging heat with the working fluid when the thermoacoustic phenomenon happens. To generate an acoustic wave, a sharp temperature drop along the length of the regenerator along its axis is essential [2], [13]. Normally, the gas displacement

(a) (b)

Figure 3.5 (a)- Cartridge type heaters (b)- K type thermocouple

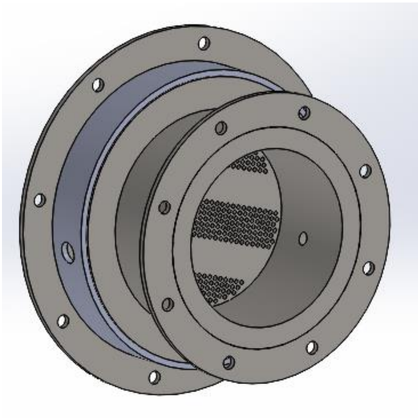

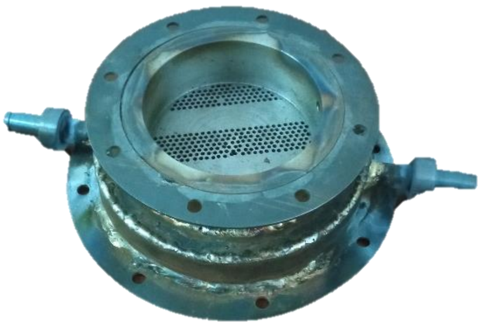

(a) (b)

Figure 3.6 3D Model of the cold heat exchanger (b) Fabricated cold heat exchanger

amplitude is expected to be a significant amount of regenerator, and It should possess a giant level of acoustic impedance [40]. Across the regenerator, a sharp temperature difference is present, and it would cause an increase in the volumetric velocity of the working fluid. Furthermore, a significant pressure drop occurs over the device's regenerator [35]. In the regenerator designing process, the porosity (Φ) and the hydraulic radius (rh) given in Equation 3.13 and Equation 3.14 are important parameters to guarantee sufficient thermal interaction between the surface of the solid parts and the working fluid in the regenerator. The hydraulic radius is typically smaller than the thermal penetration depth [39].

$$\emptyset = 1 - \frac{\pi n D_{wire}}{4} \tag{3.13}$$

$$r_h = D_{wire} \frac{\emptyset}{4(1-\emptyset)} \tag{3.14}$$

The porosity of the regenerator should be high, and it should be between 70% and 85% for optimal working conditions [41]. Heat transfer across the regenerator wall must be limited to avoid decreased system efficiency. In this research, the regenerator was made by the catalytic converter of a vehicle, as shown in Figure 3.7, and it has an 83mm diameter and consists of 1mm square haloes. During the experimental process, the regenerator length was increased from 15mm to 30mm by 5mm.

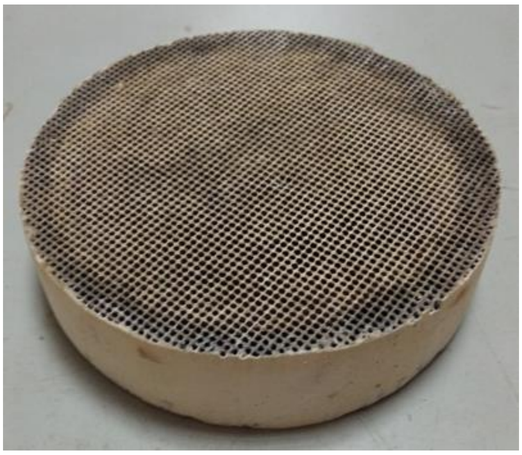

Figure 3.7 Regenerator

The thermal buffer tube serves as an insulating barrier between the HHX and the feedback network that is at the ambient temperature. To ensure sufficient thermal isolation, the thermal buffer tube should have a length no less than six times the amplitude gas displacement [34]. In this configuration, the thermal buffer tubes employed are constructed from sheet metal with a thickness of 1.6mm. These tubes exhibit a tapering diameter, gradually reducing from 83mm to 63mm while maintaining a consistent length of 250mm. The fabricated model of the core assembly is shown in Figure 3.8 below.

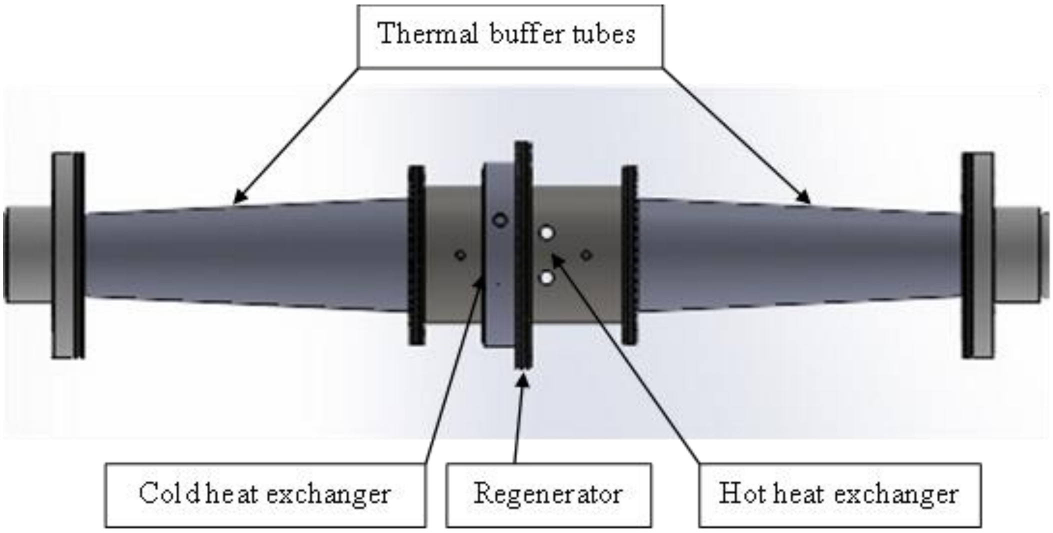

Figure 3.8 3D model and fabricated thermoacoustic core assembly

A network of pipes linking with thermal buffer tubes at CHX, without a discontinuing surface, facilitates the formation of an acoustic traveling wave within the system. This piping network system is used to guide the fundamental wave generated within the acoustic core, characterized by compliance, inertance, and resistive parts [34]. The acoustic losses can be reduced by using sleek surfaces, gentle curves, and the smallest amount of variations in cross-sectional area throughout the network. The system's operational frequency can be changed, altering the feedback piping network. In this research, the PVC pipes are used to build the acoustic network of the device. The TWTAG has an acoustic network which has 5.96 m in length and 63 mm in diameter. The frequency of the generated travelling wave is around 58Hz. The reason for maintaining the frequency around above mention value is to harness the maximum amount of energy from the acoustic wave by matching the resonance frequency of the acoustic to the electric conversion device. The 3D model and the fabricated experimental setup are shown in Figure 3.9 below.

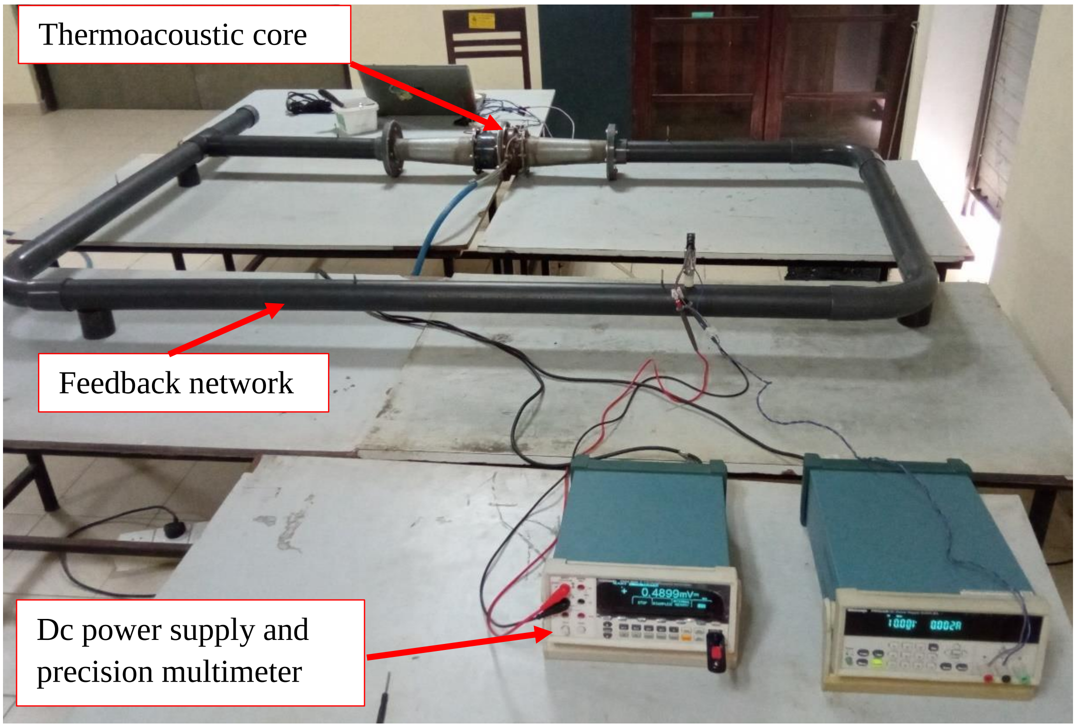

Figure 3.9 Experimental setup

The experimental setup incorporates diverse sensors and actuators for comprehensive monitoring, recording, and control of inputs and outputs. Specifically, two K-type thermocouples are used to regulate the temperatures of both the hot and cold heat exchangers. Additionally, the cold heat exchanger's inlet and outlet water temperatures are measured using another two K-type thermocouples.

Pressure sensors are deployed to gauge the pressure amplitude of the generated wave within the system, enabling the subsequent calculation of acoustic power based on these pressure amplitude values. The acoustic pressure sensors should be placed near the velocity antinodes in the acoustic feedback loop of the device to achieve optimum results [34]. Furthermore, a digital oscilloscope is utilized to ascertain the operational frequency of the system. This is achieved by measuring the frequency of the signal generated by the loudspeaker, providing valuable insights into the system's overall performance.

The efficiency of thermal-to-acoustic conversion can be calculated by getting the ratio between the thermal power that was supplied to the system and the acoustic power that was generated by the system, as given in Equation 3.15.

$$\mu = \frac{\dot{W}}{\dot{Q}_h} \tag{3.15}$$

The theoretical upper limit of thermodynamic devices is given by Carnot efficiency as given in Equation 3.16. The Carnot efficiency of thermoacoustic devices is dedicated by the temperature values of HHX and CHX where T_h and T_c are the absolute temperatures respectively.

$$\mu_{Carnot} = 1 - \frac{T_c}{T_h} \tag{3.16}$$

The efficiency of a TWTAG can be enhanced by minimizing losses such as thermal conduction, viscous dissipation and acoustic losses in the thermoacoustic core while optimizing the parameters of the device such as regenerator length, porosity and working fluid properties.

3.4.3 Experimental procedure

A systematic and repeatable testing procedure is essential for evaluating the performance of TWTAG with different regenerator and working fluid conditions. The aim of the tests is to identify the effect of the regenerator length on the performance of thermal to acoustic conversion of TWTAG under controllable working fluid conditions. In order to do that, the pressure amplitude variations of acoustic wave propagate through the device was analyzed. The experimental setup has four regenerators which has varying lengths 15 mm 20 mm, 25 mm and 30 mm each regenerator tested individually with same environmental conditions. The working fluid temperature varied by changing the temperature of HHX while the temperature of the CHX is kept constant.

Before starting the testing, pressure sensors and temperature sensors were calibrated for ensuring the accuracy and the reliability of the data acquired from them. The continuous water supply was established through the CHX to maintain a constant temperature throughout the experiment providing a stable reference point. The temperatures of cooling water at the inlet and outlet were monitored and measured.

The temperature of the working fluid is increased in controlled steps, such as 30 0C, 350C, 40 0C, 45 0C and 50 0C for each regenerator lengths under the constant atmospheric conditions. At every above-mentioned temperature values, the system has given predefined time period to become steady state conditions before the readings were recorded. The pressure amplitude values were measured using two sensor method along the feedback network at every temperature increment and the data was logged meticulously. At the end of the testing procedure for one regenerator length, waited for cooling down the system and the regenerator was replaced with the next one and this testing procedure was followed for all the other regenerator lengths.

To ensure the repeatability of the test results, is test is conducted three times for each regenerator length maintaining the identical environmental factors such as atmospheric temperature and humidity. If any deviations in the results were observed, the system and the environmental conditions were investigated and tested again if necessary. The performance of the TWTAG was analyzed by comparing the pressure amplitude values using the graphs between the pressure amplitude and working fluid temperatures.

CHAPTER 4

4 RESULTS AND DISCUSSION

4.1 Computational results

Two configurations of a hot heat exchanger underwent thorough analysis upon meticulous examination of the results derived from CAD software, and the results are illustrated in Figure 4.1 and Figure 4.2 below. The spread of high-temperature regions is prominent in configuration (a) compared to (b), indicating the even distribution of thermal energy over the heat exchanger. Under the same conditions provided, configuration (a) has a higher maximum reachable temperature than (b). It was determined that the configuration (a) emerged as the optimal choice compared to the configuration (b). The selection process was heavily influenced by considerations pertaining to the highest reachable temperature, temperature distribution, manufacturability, and material cost, which played pivotal roles in determining the final dimensions and design specifications.

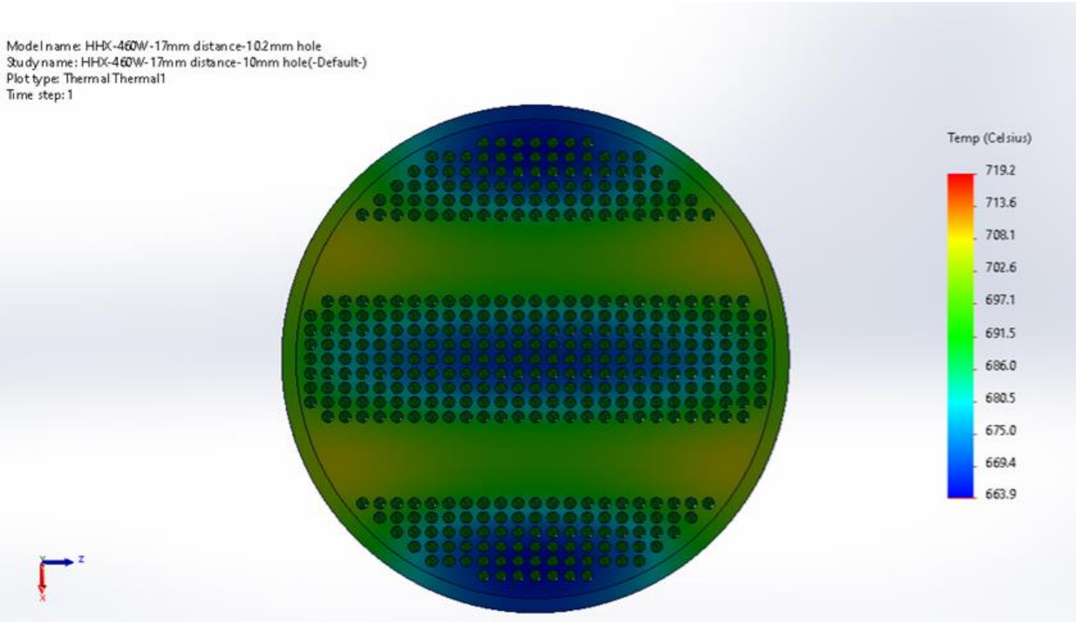

Figure 4.1 Simulation results of configuration (a)

The existing model was used to identify the sensitivity of the parameters of the thermoacoustic generator. The simulation primarily concentrated on assessing how variations in the length of the chosen regenerator and the ambient temperature impact the device's efficiency when subjected to standard pressure conditions. The outcomes derived from the simulation have been visually illustrated in Figure 4.3 to Figure 4.5. The variation of the pressure amplitude at varying thermal conditions of working fluid with the regenerator length is shown in Figure 4.3 below. There is an increment of the pressure amplitude with the length of the regenerator and the working fluid temperature within the given range. The rate of increase varies in pressure amplitudes, showing steeper curves with the higher working fluid temperatures. Figure 4.4 illustrates the relationship between the volume flow rate and regenerator length at varying thermal conditions of the working fluid, and the same pattern is shown here also. At the high temperatures of the working fluid, the volume flow rate is higher for a given regenerator length. The efficiency of the conversion process of thermal energy into acoustic energy with the variation of regenerator length and working fluid temperature is depicted in Figure 4.5.

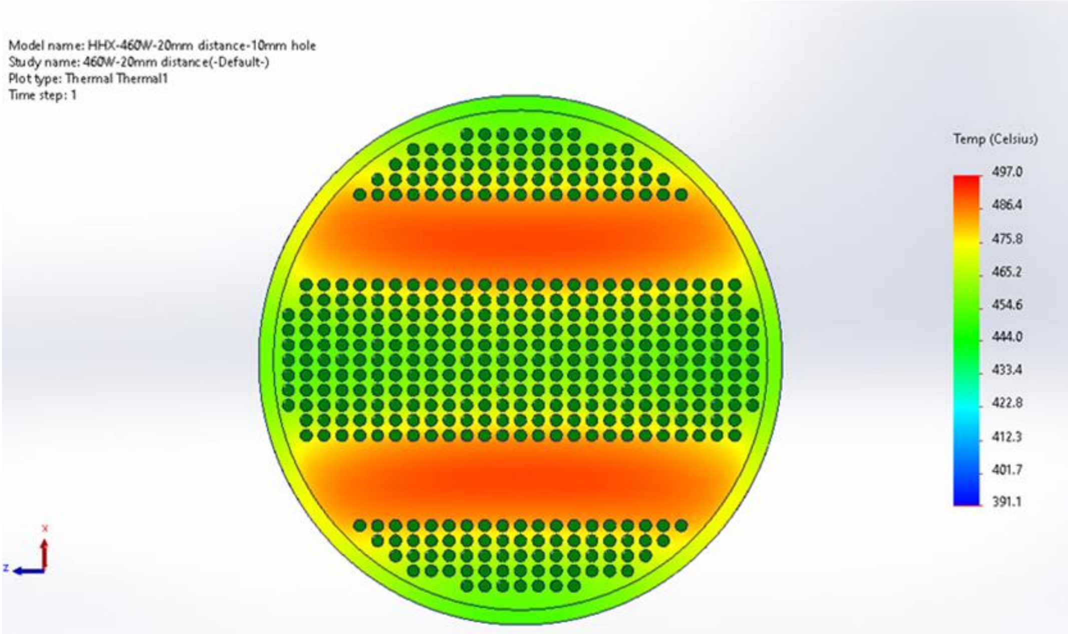

Figure 4.3 Simulation results of configuration (b)

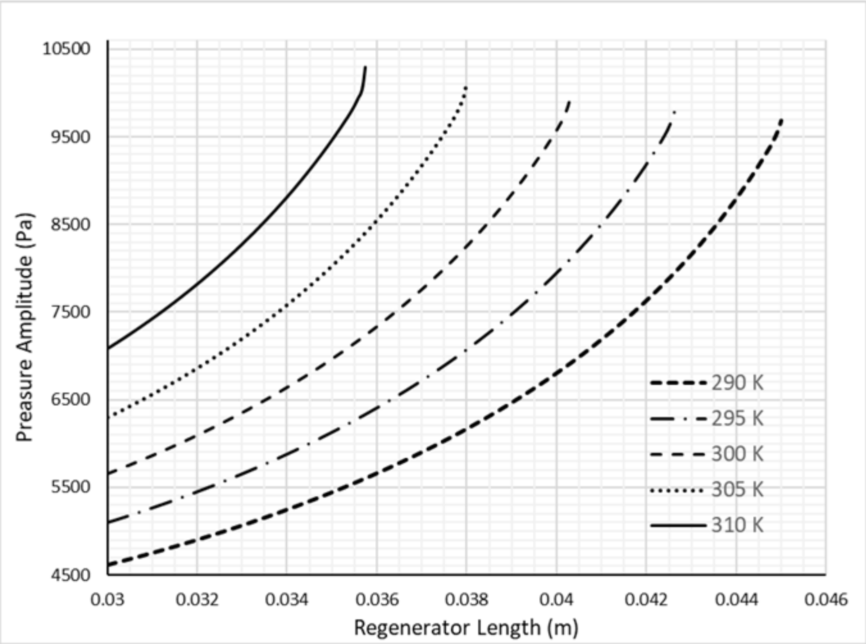

Figure 4.2 Variation of pressure amplitude with regenerator length under different working fluid temperature

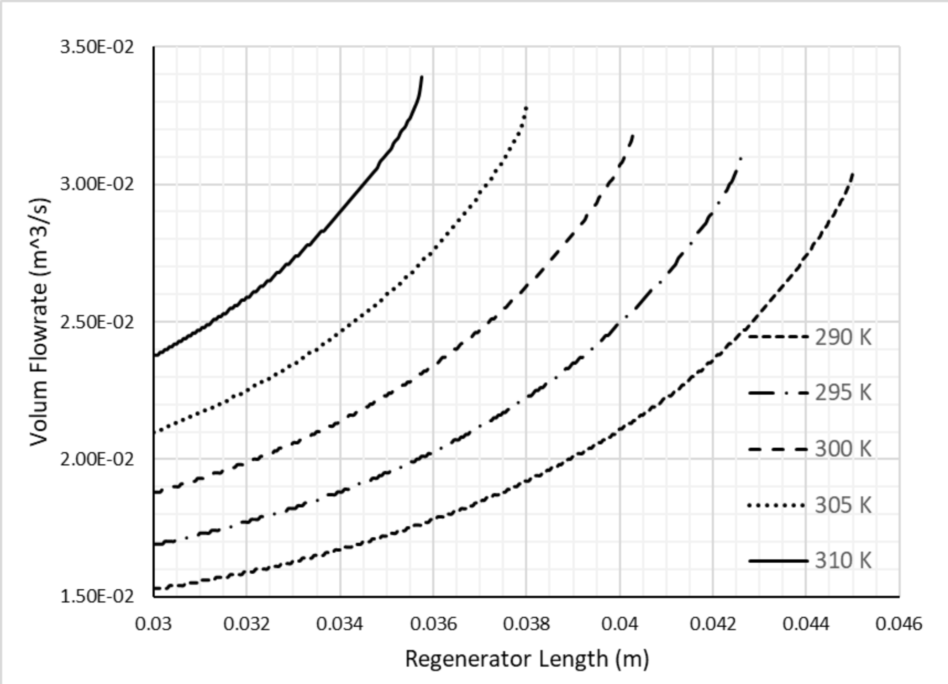

Figure 4.5 Variation of volume flowrate amplitude with regenerator length under different working fluid temperature

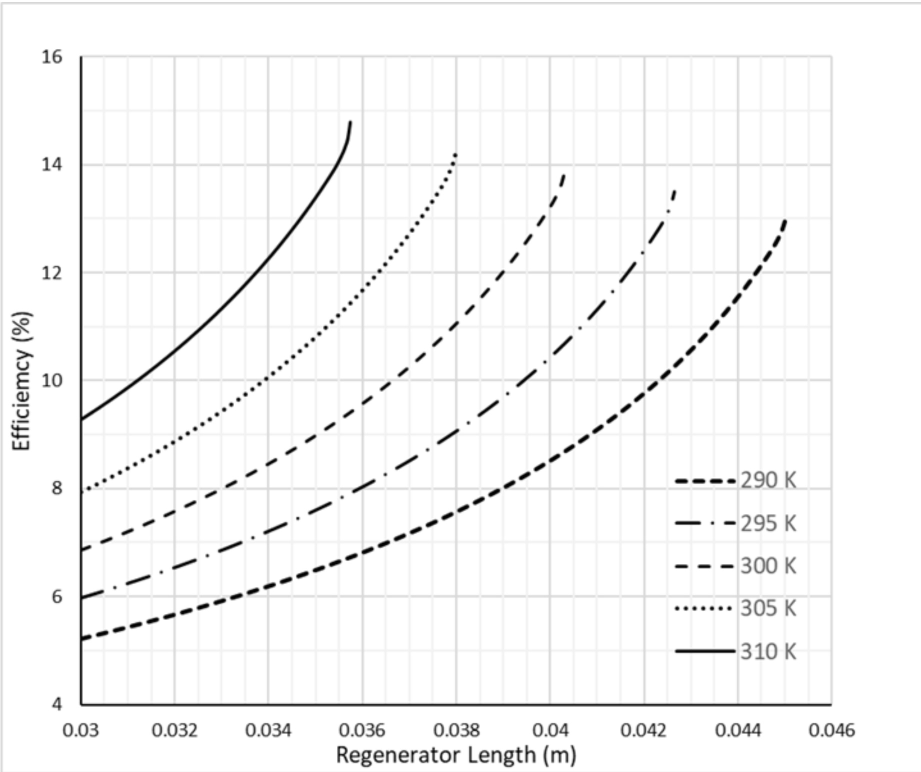

Figure 4.4 Thermal to acoustic conversion efficiency with regenerator length under different working fluid temperature

The results showed a significant change in pressure amplitude, volume flowrate amplitude, and device efficiency. Several observations could be made on the graphs. For a given ambient temperature of the working fluid, the pressure amplitudes, the volume velocities, and the efficiencies increase with the regenerator length. Further, there is a limit for the regenerator length, beyond which the simulation does not show acoustic phenomena. The results show a steep drop in pressure amplitudes along the regenerator, which suggests that the optimal length must balance the pressure and heat transfer requirements to maximize the overall efficiency of the system and the acoustic phenomenon [1]. According to Swift's findings, the longer regenerator increases the surface area for heat transfer and also introduces additional thermal and viscous losses to the system [34]. The increment of the thermal and viscous losses could be the reason for the vanishing of the acoustic phenomenon of the system. Similarly, when the working fluid temperature is increased for a constant regenerator length, the pressure amplitudes, the volume flowrate amplitude, and the efficiencies increase up to a limit. Furthermore, considering the performance indicators, i.e., pressure amplitude, volume flowrate amplitude, and efficiency, the maximum reachable value increases with the increasing temperature of the working fluid.

Figure 4.6 shows the variation of pressure amplitude and volume flow rate amplitude of working fluid as a function of the regenerator diameter of TWTAG. The pressure amplitude and the volume flowrate amplitude decrease with the increment of the regenerator diameter up to a particular value and then increase with the diameter within the selected range.

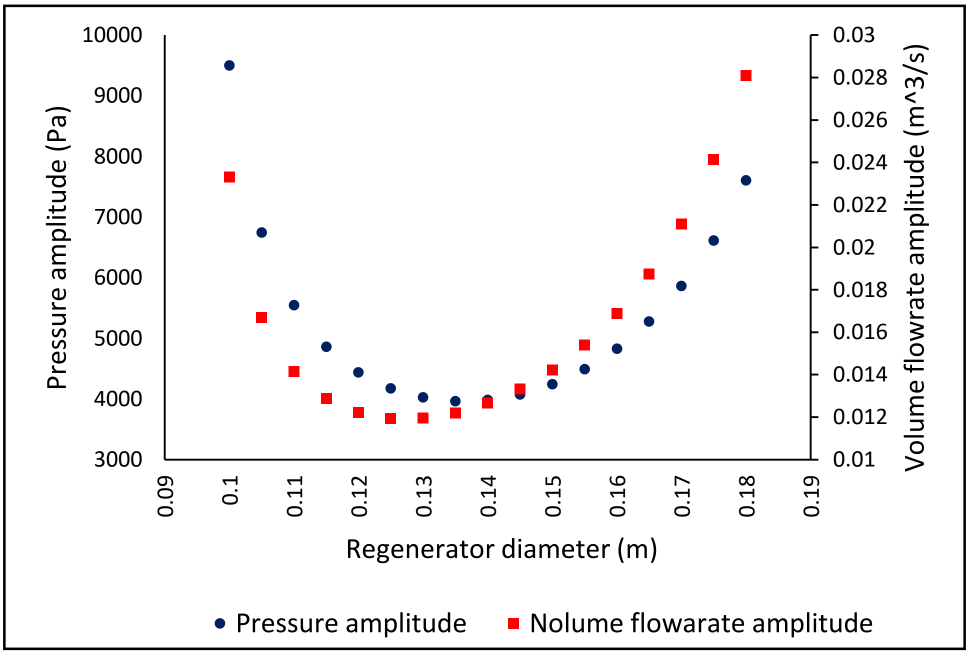

Figure 4.6 Pressure amplitude and the volume flowrate amplitude variation of the device with the regenerator diameter

Figure 4.7 illustrates the relationship between heat input at the HHX and thermal to acoustic conversion efficiency of the device as a function of the regenerator diameter of the device. According to the graph, although the heat input decreases initially, that increases with the diameter of the device after giving the minimum value. The larger diameters offer a progressively lower efficiency.

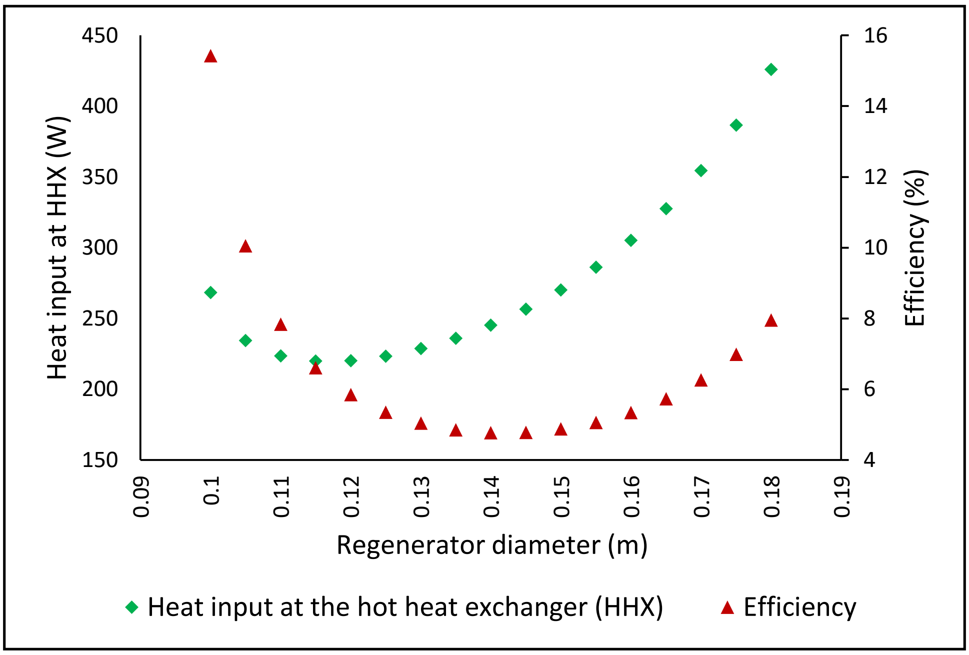

Figure 4.7 Amount of heat input at the hot heat exchanger and the efficiency of the device variation with the regenerator diameter

The above simulations were focused on the effect of the regenerator diameter on the efficiency of the thermoacoustic generator. Figure 4.6 and Figure 4.7 show the results obtained during the simulations. According to the results and analysis, the design parameters, such as the diameter of the regenerator, have a huge impact on the performance of TWTAG. The regenerator with a 0.135 m diameter gave the minimum pressure amplitude. In addition, the minimum value of the volume flow rate amplitude was given by the regenerator with a 0.125 m diameter. The volume flow rate and pressure amplitude increase by increasing or decreasing the regenerator diameter from the point that gives minimum values. The regenerator, which has a 0.14 m diameter, gave the minimum efficiency. However, the diameter which has given the minimum efficiency is greater than the diameter which has given the minimum heat addition of the hot heat exchanger. Moreover, maximum efficiency can be achieved by changing the diameter of the regenerator. The small diameters offer the highest efficiency within the range due to the lower heat input at the hot heat exchanger.

4.2 Experimental results

The experimental setup was tested under different regenerator lengths and different ambient conditions. The amplitude of pressure and acoustic power generated by the TWTAG relies on the amount of thermal energy transferred to the device. However, the maximum allowable amount of thermal energy supplied to the system is governed by the highest service temperature of the heaters rather than their maximum rated power. Also, the maximum temperature that the HHX can reach depends on the thermal-to-acoustic conversion rate and heat loss. The pressure sensors installed into the feedback network of the thermoacoustic engine can be employed to compare pressure amplitudes obtained through experimentation with those simulated.

Figure 4.8 illustrates the variation of the temperatures of HHX and CHX as a function of time during the experiments with regenerator which has 15 mm diameter. According to the graph, it has taken more time to reach a steady state due to the lower wattage of the cartridge-type heat exchanger and also the heat losses. The temperatures of both heat exchangers start at room temperature. The temperature of the HHX gradually increases over time, with a steady rise observed until the 1950 seconds. After that, there is a sudden increment in the temperature of HHX, and after that, the temperature stabilizes around 280 ^{0}C. There is a slight increment in the temperature of CHX from the start to 1950 seconds due to the heat transfer through the regenerator wall and the working fluid from HHX to CHX. After that time, the temperature of CHX also shows the same relationship as the HHX, stabilizing around 60 ^{0}C. The sharp increment in temperature of both heat exchangers started after the start of the propagation of acoustic waves through the device. Therefore, 194 ^{0}C can be considered as the onset temperature difference of this condition. After the start of the propagation of acoustic waves, the heat transfer rate from HHX to CHX is increased significantly.

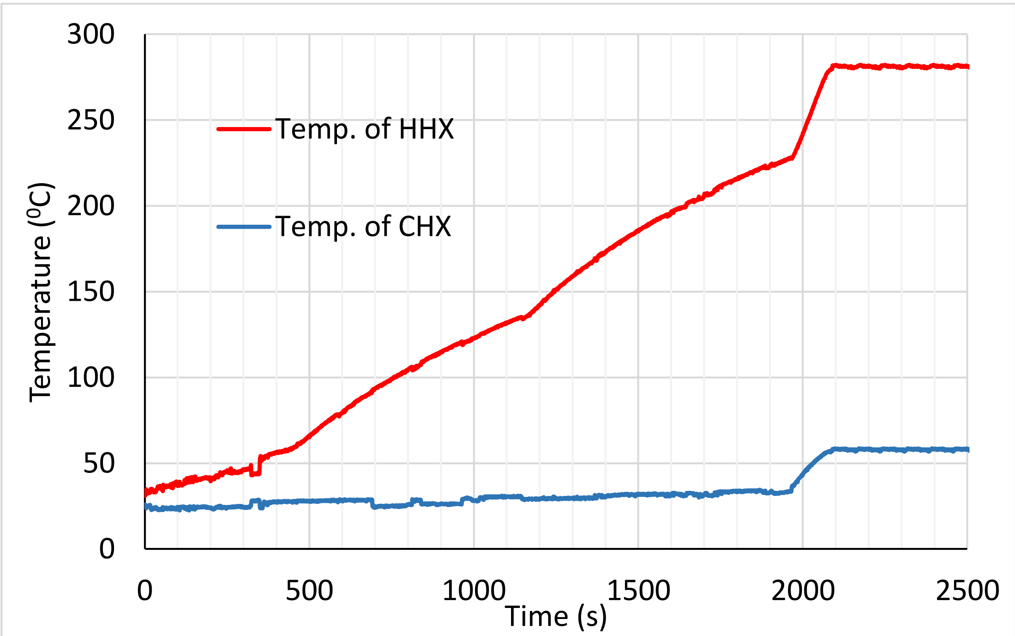

Figure 4.8 variation of the temperatures of HHX and CHX with the time

A significant amount of change in onset temperature difference was not observed during the testing procedure of the other regenerators.

The inlet temperature and outlet temperature of the cooling water of CHX are visualized in Figure 4.9, given below. The temperature of the cooling water at water inlet alters slightly around 27-25 ^{0}C, and it remains nearly constant throughout the observation. The outlet temperature of the cooling water of CHX rises gradually from the start to 2000 seconds and then shows a sharp rise to around 36 ^{0}C. Then, it tends to stabilize throughout the experiment. From the previous graph, there is a sudden increment in the temperature of CHX, and because of that, the temperature of the cooling water circulated through it also gets high.

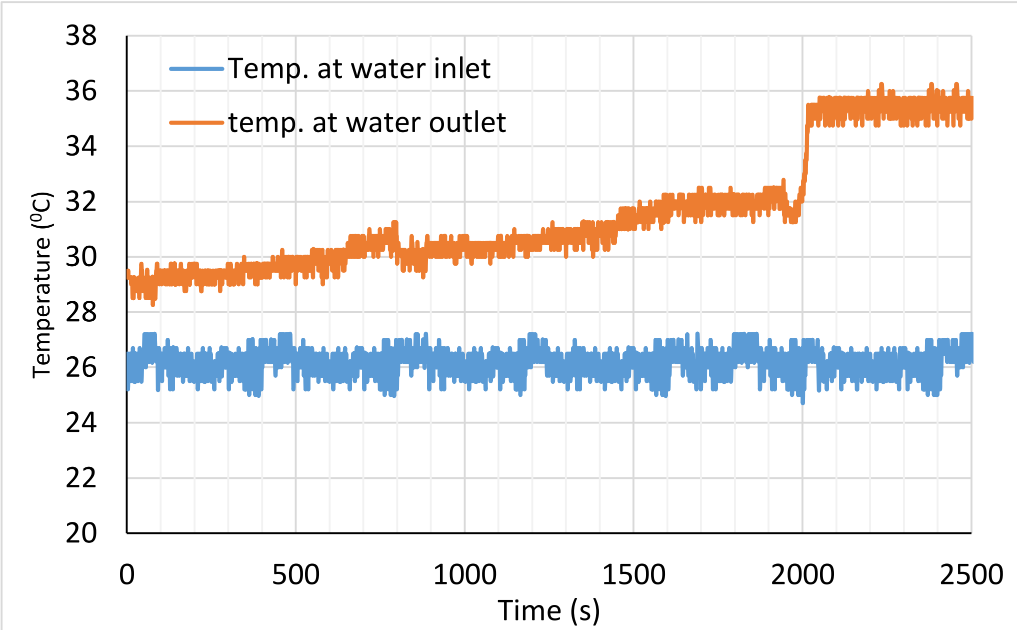

Figure 4.9 Variation of the temperature of cooling water at the inlet and outlet of CHX with time

Figure 4.10 illustrates the experimental results extracted from the TWTAG, which that the variation of the pressure amplitude with different regenerator lengths under different working fluid temperatures. The length of the regenerator has been increased from 15 mm to 30 mm by 5 mm while maintaining constant diameter. The graph demonstrates a clear trend where increasing the working fluid temperature leads to a higher-pressure amplitude for all the regenerators. The data points include error bars representing standard deviation, providing insight into the variability of measurements and experimental uncertainty during the tests. The results indicate that the 30 mm regenerator produces the highest pressure amplitude across all temperature conditions within this length range, suggesting that a longer regenerator enhances performance by improving heat transfer and interaction with the oscillating working fluid. Further, there is a limit for the regenerator length that offers highest pressure amplitude due to increment of acoustic and thermal losses within the system with the length of the regenerator. However, the overlap in error bars at certain points suggests that differences between regenerator lengths may not always be statistically significant, warranting further investigation. Additionally, while all configurations follow a

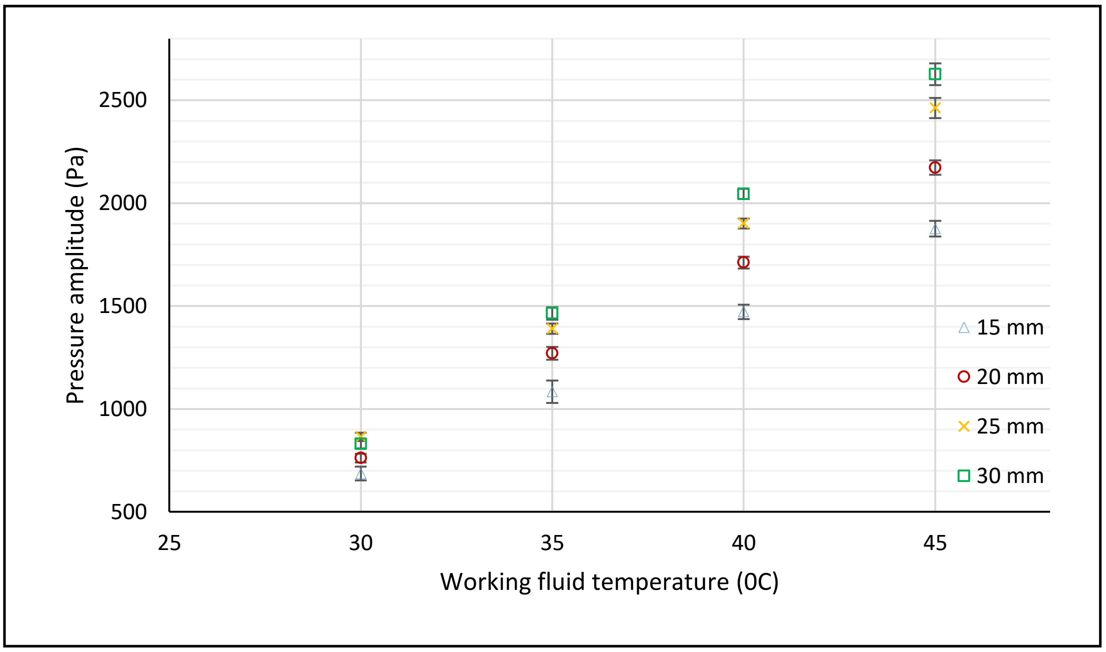

Figure 4.10 Experimental results

similar increasing trend, the rate of pressure amplitude increase appears to be more pronounced at higher temperatures, which could be attributed to non-linear effects in thermoacoustic energy conversion. Furthermore, future work should consider additional experimental trials to reduce uncertainty and validate the observed trends.

4.3 Discussions of validation process of experimental and computational results

Figure 4.10 illustrates the contrast of the findings gathered from simulations of DeltaEC and the actual pressure values coming from the experimental setup. The pressure amplitude measurements obtained through experimentation align with the results obtained from simulations, affirming the computational model's reliability for forecasting results. The validation between experimental data and the simulated data using DeltaEC was a primary objective of this research. The experimental setup was tested under different regenerator lengths and different working fluid conditions. The amplitude of acoustic power and pressure produced by the TWTAG relies on the amount of thermal energy transferred to the device. However, the maximum allowable amount of thermal energy supplied to the system is governed by the highest service temperature of the heaters rather than their maximum rated power. The acoustic sensor installed into the piping network of the thermoacoustic engine can be employed to compare pressure amplitudes obtained through experimentation with those simulated.

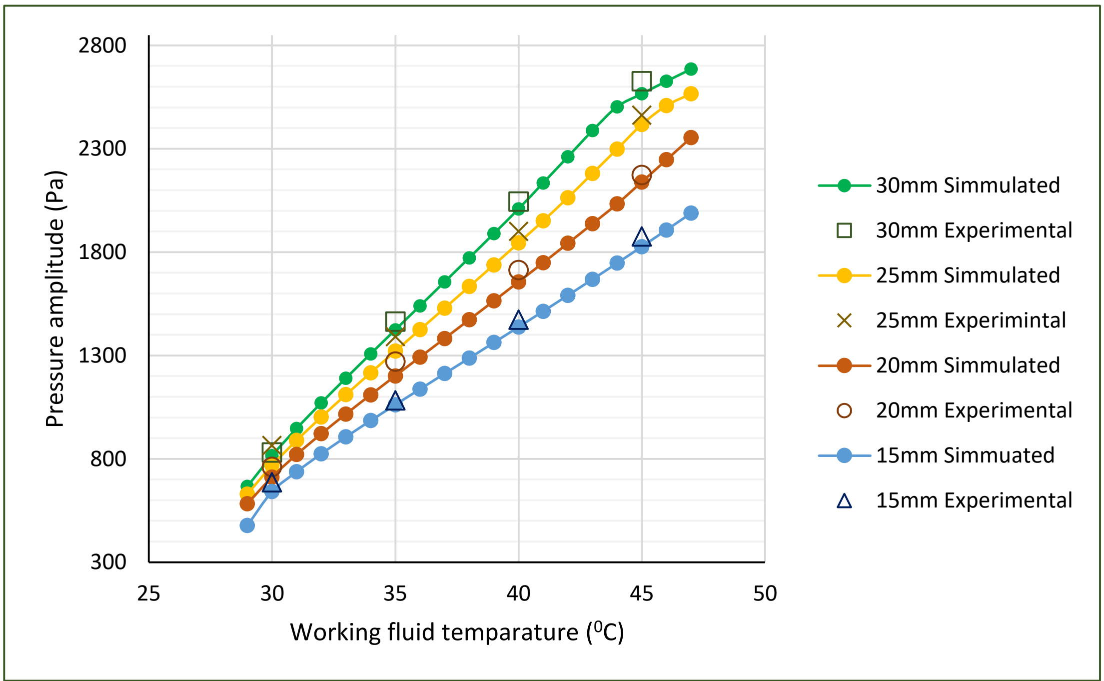

Figure 4.11 Comparison of simulated and experimental data with different regenerator lengths

The results and analysis indicate a clear connection between the temperature of the working fluid and key characteristics of the traveling wave thermoacoustic generator, such as pressure amplitude and volume flowrate amplitude. As the working fluid temperature increases, there is a noticeable rise in both pressure amplitude and volume flowrate amplitude, along with an improvement in efficiency, all while maintaining a constant regenerator length. Furthermore, higher working fluid temperatures lead to the possibility of achieving greater efficiency with shorter regenerator lengths. If the working fluid temperature increases by 1 degree Celsius while maintaining the regenerator length constant, the pressure amplitude increases by 6.2%. Consequently, the length of the regenerator is inversely related to the maximum achievable outcome, and it is apparent that a maximum limit to efficiency exists for a given working fluid temperature. The TWTAG was observed on different regenerator lengths with a 460W maximum heat input at the HHX and under varying thermal conditions of the working fluid. The acoustic power and the pressure amplitude of the acoustic wave generated in the device rely on the amount of heat supplied to the system. Considering these factors and the data extracted from the experimental setup, the calculated maximum thermal-to-acoustic conversion efficiency of this TWTAG is 6.8 %. The maximum conversion efficiency of each configuration is increased with the working fluid temperature. Additionally, simulation results also demonstrate a positive correlation between regenerator length and efficiency.

For all the regenerator lengths, both experimental and simulated values follow a trend of liner increasing, indicating a proportional relationship between working fluid temperature and pressure amplitude. The pattern of the graphs suggest that a longer regenerator enhances pressure amplitude by improving thermoacoustic energy conversion efficiency within the same conditions. For the regenerator which has 15 mm length, a linear equation of the experimental data is provided as follows.

$$P_1 = 79.131T - 1687.9 \tag{4.1}$$

Where P_1 represents the pressure amplitude in Pa and T represents the working fluid temperature in ^{0}C. According to the equation, for every 1^0C increase in working fluid temperature, the pressure amplitude of the travelling wave increases by approximately 79.131 Pa. The negative intercept of the equation suggesting that the system would not sustain significant pressure amplitude bellow a certain temperature level.

The pressure amplitude measurements obtained through experimentation closely align with the simulated pressure amplitude distributions with minor deviations, affirming the reliability of the DeltaEC model developed during the research for predictive purposes of thermoacoustic generators under various operating conditions. The minor deviations can be ascribed to experimental errors such as the ambient conditions' variation and the sensor values' precision. The simulated results are consistently higher than the experimental data, likely due to idealized conditions in simulations that do not fully account for real-world losses, such as thermal and acoustic dissipation.

CHAPTER 5

5. CONCLUSION

This research aims to investigate and analyze the performance of TWTAG with the variation of key parameters using a computational model and an experimental setup. The results of the present study provide a clear indication of TWTAGs based on the conditions of working fluid and the regenerator dimensions. According to the data validated through the experiments and DeltaEC model, the length of the regenerator and the working fluid temperature significantly impact the pressure amplitude, volume flow rate amplitude, and device efficiency. Higher efficiencies of the traveling wave thermoacoustic generator can be achieved by increasing the regenerator length, but there is a limit that defines the maximum efficiency for a given condition. Further, the desired efficiency can be achieved with shorter regenerator lengths for higher working fluid temperatures. The experimental data indicate that the device achieved a maximum efficiency of 6.8%, converting thermal energy to acoustic energy at a rate of 3.12 W. In comparison, the Carnot efficiency of the device is 44.04%, highlighting the potential for further optimization of energy conversion efficiency in future work. This study could be useful for selecting the length of the regenerator to design a thermoacoustic engine with higher performance.

The aforementioned efficiency limit is caused by not having the expected acoustic behavior beyond the certain regenerator length for a given working fluid temperature. Furthermore, in the selected range of the diameter of the regenerator, there is a value that gives a minimum efficiency of the device. The performance of the thermoacoustic engine is increased either by increasing or decreasing the regenerator diameter from the point that gives minimum efficiency. The excessive length and diameter introduce thermal and viscous losses, limiting the device's acoustic phenomenon.

It verifies that the DeltaEC model developed during this research is accurate since experimental measurements of pressure amplitude are in strong concurrence with the results comming from the computer simulations. The minor deviations happened due to experimental variances such as sensor precision and fluctuation in the ambient conditions. In summary, this work demonstrated that maximization of the efficiency of traveling wave thermoacoustic generators requires optimization of both regenerator dimensions and working fluid conditions; besides, the DeltaEC model represents an acceptable predictive tool for further studies in thermoacoustic generation.

Although this study validated the DeltaEC model with the experimental setup and provided useful information regarding the performance of the traveling wave thermoacoustic generator, several limitations need to be focused on in future studies. The fixed working fluid conditions used in the study are among those. Changing the type of working fluid, pressure of the working fluid, and temperature will achieve different test conditions, especially during practical applications where the working fluid conditions are ever-changing. Moreover, the study was concerned with only a limited range of lengths and diameters of the regenerators due to considering the availability and the cost. Extending a larger range of regenerator dimensions and participating in other geometrical parameters, such as the porosity and roughness of the regenerator, may yield even better performance.

When comparing the performance of our device to state-of-the-art thermoelectric generators (TEGs), several key differences emerge. TEGs typically achieve efficiencies ranging from 5% to 8% while maintaining the temperature of the hot side around 580K and the temperature of the cold side at 300 K. The efficiency depends on the temperature difference between the hot and cold sides of the TEGs[42]. Furthermore, unlike TEGs, which primarily convert thermal energy directly into electrical energy, TWTAG utilizes acoustic energy, opening new avenues for applications in low-grade heat recovery. Not only the electricity, the energy that is harnessed by the TWTAG can be converted into mechanical energy using a moving piston frictionless sterling engine [29]. As parallel technologies evolve, optimizing our device's design and operational parameters could position it favorably in the energy conversion landscape, particularly for niche applications where thermoelectric solutions may not be as effective.

During the study, the fabrication process of the experimental setup faced challenges related to the availability of suitable materials, tools, and machine technologies due to the worst economic situation in the country. Fabricating heat exchangers using low-heat conductive materials potentially affects the heat transfer rate and the device's efficiency. Moreover, developing the data acquisition system took time due to challenges in sourcing appropriate sensors and actuators. Future studies could utilize advanced machine operations and materials to improve the performance of TWTAG.

5.1 Future works

Future studies should also be directed towards investigating greater heat exchanger designs for thermoacoustic generators because the same design was considered for both hot and cold heat exchangers during this study. Advanced materials and configuration in heat exchangers contribute to their overall efficiency. Utilizing different working fluids, such as inert gases in different pressure and temperature conditions, may increase the efficiency of the device. The thermal to acoustic conversion is only studied during research. The study can be further extended to analyze the acoustic-to-electric conversion performance by developing a conversion device. Finally, the measurement uncertainties could be reduced, and more accurate computational model validation will be provided by using an experimental setup with higher precision and control.

PUBLICATIONS

- MDA. Wickramasinghe, MMID. Manthilake, MA. Wijewardane, and RACP. Ranasinghe, “Computational Analysis on the Influence of Design Parameters and Ambient Conditions on Performance of Single Stage Traveling Wave Thermoacoustic Generator,” *Moratuwa Engineering Research Conference, MERCon*, pp. 288–291, 2023, doi: 10.1109/mERCon60487.2023.10355520.

- MDA. Wickramasinghe, MMID. Manthilake, MA. Wijewardane, and RACP. Ranasinghe, “Numerical Study of Single Stage Travelling Wave Thermoacoustic Generator Through Regenerator Optimization” 17th KDU International Research Conference 2024, https://irc.kdu.ac.lk/2024/documents/17th-irc-programme-book-2024.pdf

REFERENCES

[1] GW Swift, “Thermoacoustic engines,” *Acoustical Society of America*, no. July 1988, 1988.

[2] M. Mcgaughy, “Design and Analysis of a Single Stage, Traveling Wave, Thermoacoustic Engine for Bi-Directional Turbine Generator Integration,” 2018.

[3] S. Somu, D. Lacoste, S. Saxena, W. L. Roberts, and R. M. Keolian, “Design Optimization of a Multi-kW Thermoacoustic Electric Generator Using DeltaEC Model,” in *Volume 5: Controls, Diagnostics, and Instrumentation; Cycle Innovations; Cycle Innovations: Energy Storage*, American Society of Mechanical Engineers, Sep. 2020. doi: 10.1115/GT2020-15419.

[4] P. Saechan and A. J. Jaworski, “Thermoacoustic cooler to meet medical storage needs of rural communities in developing countries – High pressure system,” *Thermal Science and Engineering Progress*, vol. 8, pp. 31–46, 2018, doi: 10.1016/j.tsep.2018.07.010.

[5] D.-H. Li, Y.-Y. Chen, E.-C. Luo, and Z.-H. Wu, “Study of a liquid-piston traveling-wave thermoacoustic heat engine with different working gases,” *Energy*, vol. 74, pp. 158–163, Sep. 2014, doi: 10.1016/j.energy.2014.05.034.

[6] A. Al-Kayiem and Z. Yu, “Numerical investigation of a looped-tube traveling-wave thermoacoustic generator with a bypass pipe,” *Energy Procedia*, vol. 142, pp. 1474–1481, Dec. 2017, doi: 10.1016/j.egypro.2017.12.595.

[7] C. Iniesta, J. L. Olazagoitia, J. Vinolas, and J. Aranceta, “Review of travelling-wave thermoacoustic electric-generator technology,” *Proceedings of the Institution of Mechanical Engineers, Part A: Journal of Power and Energy*, vol. 232, no. 7, pp. 940–957, Nov. 2018, doi: 10.1177/0957650918760627.

[8] P. H. M. W. Panhuis, “Mathematical aspects of thermoacousticse,” Eindhoven University of Technology, Eindhoven, Netherlands, 2009.

[9] RAYLEIGH, “THE EXPLANATION OF CERTAIN ACOUSTICAL PHENOMENA 1,” *Nature*, vol. 18, no. 455, pp. 319–321, Jul. 1878, doi: 10.1038/018319a0.

[10] P. H. Ceperley, “A pistonless Stirling engine—The traveling wave heat engine,” *J Acoust Soc Am*, vol. 66, no. 5, pp. 1508–1513, Nov. 1979.

[11] K. O. A. Abdoulla-Latiwish, X. Mao, and A. J. Jaworski, “Thermoacoustic micro-electricity generator for rural dwellings in developing countries driven by waste heat from cooking activities,” *Energy*, vol. 134, pp. 1107–1120, 2017, doi: 10.1016/j.energy.2017.05.029.

[12] M. Wickramasinghe, M. Manthilake, M. Wijewardane, and R. Ranasinghe, “Computational Analysis on the Influence of Design Parameters and Ambient

Conditions on Performance of Single Stage Traveling Wave Thermoacoustic Generator," *Moratuwa Engineering Research Conference, MERCon*, pp. 288–291, 2023, doi: 10.1109/mERCon60487.2023.10355520.

[13] J. P. Clark, W. C. Ward, and G. W. Swift, "Design environment for low-amplitude thermoacoustic energy conversion (DeltaEC)," *J Acoust Soc Am*, vol. 122, no. 5, p. 3014, 2007.

[14] N. M. Hariharan, P. Sivashanmugam, and S. Kasthurirengan, "Influence of stack geometry and resonator length on the performance of thermoacoustic engine," *Applied Acoustics*, vol. 73, no. 10, pp. 1052–1058, 2012, doi: 10.1016/j.apacoust.2012.05.003.

[15] C. N. Markides, A. Osuolale, R. Solanki, and G. B. V. Stan, "Nonlinear heat transfer processes in a two-phase thermofluidic oscillator," *Appl Energy*, vol. 104, pp. 958–977, 2013, doi: 10.1016/j.apenergy.2012.11.056.

[16] I. B. Gorshkov and V. V. Petrov, "Experimental study of an annular four-stage thermoacoustic engine with a traveling wave," *Image Journal of Advanced Materials and Technologies*, vol. 7, no. 2, pp. 149–158, 2022, doi: 10.17277/jamt.2022.02.pp.149-158.

[17] J. R. Brewster, R. Raspet, and H. E. Bass, "Temperature discontinuities between elements of thermoacoustic devices," *J Acoust Soc Am*, vol. 102, no. 6, pp. 3355–3360, 1997, doi: 10.1121/1.419578.

[18] R. S. Wakeland and R. M. Keolian, "Effectiveness of parallel-plate heat exchangers in thermoacoustic devices," *J Acoust Soc Am*, vol. 115, no. 6, pp. 2873–2886, 2004, doi: 10.1121/1.1710503.

[19] A. Piccolo and G. Pistone, "Estimation of heat transfer coefficients in oscillating flows: The thermoacoustic case," *Int J Heat Mass Transf*, vol. 49, no. 9–10, pp. 1631–1642, 2006, doi: 10.1016/j.ijheatmasstransfer.2005.11.009.

[20] L. K. Tartibu, "Developing more efficient travelling-wave thermo-acoustic refrigerators: A review," *Sustainable Energy Technologies and Assessments*, vol. 31, no. December 2018, pp. 102–114, 2019, doi: 10.1016/j.seta.2018.12.004.

[21] A. Hamood, A. J. Jaworski, and X. Mao, "Development and Assessment of Two-Stage Thermoacoustic Electricity Generator," *Energies (Basel)*, vol. 12, no. 9, p. 1790, May 2019, doi: 10.3390/en12091790.

[22] W. Kisha, P. Riley, J. McKechnie, and D. Hann, "Asymmetrically heated multi-stage travelling-wave thermoacoustic electricity generator," *Energy*, vol. 235, p. 121312, Nov. 2021, doi: 10.1016/j.energy.2021.121312.

[23] K. O. A. Abdoulla-Latiwish and A. J. Jaworski, "Two-stage travelling-wave thermoacoustic electricity generator for rural areas of developing countries," *Applied Acoustics*, vol. 151, pp. 87–98, Aug. 2019.

[24] H. Pan, D. Sun, and Z. Jie, “Multi-stage traveling-wave thermoacoustic power generation system utilizing LNG cold exergy and low-temperature waste heat,” *Appl Energy*, 2019.

[25] M. McGaughy, E. Boessneck, T. Salem, and J. Wagner, “Critical design elements for traveling wave thermoacoustic engines,” *American Society of Mechanical Engineers, Power Division (Publication) POWER*, vol. 1, pp. 1–11, 2018.

[26] A. W. Avent and C. R. Bowen, “Principles of thermoacoustic energy harvesting,” *European Physical Journal: Special Topics*, vol. 224, no. 14–15, pp. 2967–2992, 2015, doi: 10.1140/epjst/e2015-02601-x.

[27] J. Chi, J. Xu, L. Zhang, Z. Wu, J. Hu, and E. Luo, “Study of a gas-liquid-coupled heat-driven room-temperature thermoacoustic refrigerator with different working gases,” *Energy Convers Manag*, vol. 246, no. August, p. 114657, 2021, doi: 10.1016/j.enconman.2021.114657.

[28] M. A. G. Timmer, K. de Blok, and T. H. van der Meer, “Review on the conversion of thermoacoustic power into electricity,” *J Acoust Soc Am*, vol. 143, no. 2, pp. 841–857, 2018, doi: 10.1121/1.5023395.

[29] T. Biwa, T. Watanabe, and G. Penelet, “Flywheel-based traveling-wave thermoacoustic engine,” *Appl Phys Lett*, vol. 117, no. 24, p. 243902, Dec. 2020, doi: 10.1063/5.0022315.

[30] “Investigation of Travelling-wave Thermoacoustic Engines with Different Configurations By Ali Abbas Hameed Al-Kayiem BSc & MSc,” 2017.

[31] H. M. D. P. Herath, M. A. Wijewardane, and R. A. C. P. Ranasinghe, “Numerical model-based prediction of performance of single stage traveling wave thermo-acoustic engines,” *Energy Reports*, vol. 7, no. May, pp. 53–59, 2021.

[32] P. Joseph, *Understanding Acoustics: An Experimentalist’s View of Acoustics and Vibration* , vol. 70, no. 10. 2017. doi: 10.1063/pt.3.3730.

[33] T. Jin, R. Yang, Y. Wang, Y. Feng, and K. Tang, “Acoustic field characteristics and performance analysis of a looped travelling-wave thermoacoustic refrigerator,” *Energy Convers Manag*, vol. 123, pp. 243–251, 2016, doi: 10.1016/j.enconman.2016.06.041.

[34] R. M. Keolian, S. L. Garrett, and S. L. Garrett, “Thermoacoustics: A Unifying Perspective for Some Engines and Refrigerators, Second Edition,” *J Acoust Soc Am*, vol. 143, no. 4, pp. 2110–2110, 2018, doi: 10.1121/1.5031020.

[35] Z. Yu, A. J. Jaworski, and S. Backhaus, “Travelling-wave thermoacoustic electricity generator using an ultra-compliant alternator for utilization of low-grade thermal energy,” *Appl Energy*, vol. 99, pp. 135–145, Nov. 2012, doi: 10.1016/j.apenergy.2012.04.046.

[36] N. Rott, *Thermoacoustics*, vol. 20, no. C. Zurich, Switzerland: Advances in Applied Mechanics, 1980.

[37] G. Chen, L. Tang, B. Mace, and Z. Yu, "Multi-physics coupling in thermoacoustic devices: A review," *Renewable and Sustainable Energy Reviews*, vol. 146, no. March, p. 111170, 2021, doi: 10.1016/j.rser.2021.111170.

[38] S. Backhaus and G. W. Swift, "A thermoacoustic-Stirling heat engine: Detailed study," 2000. [Online]. Available: http://asadl.org/terms

[39] A. Kruse, T. Schmiel, and M. Tajmar, "Experimental validation of a looped-tube thermoacoustic engine with a stub for tuning acoustic conditions," *Energy Convers Manag*, vol. 177, no. September, pp. 292–305, 2018, doi: 10.1016/j.enconman.2018.09.069.

[40] M. E. H. Tijani and S. Spoelstra, "A high performance thermoacoustic engine," *J Appl Phys*, vol. 110, no. 9, 2011, doi: 10.1063/1.3658872.

[41] A. S. Abduljalil, Z. Yu, and A. J. Jaworski, "Selection and experimental evaluation of low-cost porous materials for regenerator applications in thermoacoustic engines," *Mater Des*, vol. 32, no. 1, pp. 217–228, Jan. 2011, doi: 10.1016/j.matdes.2010.06.012.

[42] M. A. Zoui, S. Bentouba, J. G. Stocholm, and M. Bourouis, "A review on thermoelectric generators: Progress and applications," Jul. 01, 2020, *MDPI AG*. doi: 10.3390/en13143606.